

1 **Human Cytomegalovirus IE1 Protein Disrupts Interleukin-6 Signaling by Sequestering**  
2 **STAT3 in the Nucleus**

3  
4 Justin M. Reitsma,<sup>1,2</sup> Hiromi Sato,<sup>1,4</sup> Michael Nevels,<sup>3</sup> Scott S. Terhune<sup>1,2#</sup> and Christina  
5 Paulus<sup>3#</sup>

6 1. Department of Microbiology and Molecular Genetics, Medical College of Wisconsin,  
7 Milwaukee, WI 53226, USA

8 2. Biotechnology and Bioengineering Center, Medical College of Wisconsin, Milwaukee, WI  
9 53226, USA

10 3. Institute for Medical Microbiology and Hygiene, University of Regensburg, D-93053  
11 Regensburg, Germany

12 4. Center for Infectious Disease Research, Medical College of Wisconsin, Milwaukee, WI  
13 53226, USA

14  
15 <sup>#</sup>Both authors made equal senior author contributions to this work.

16 Contact: sterhune@mcw.edu christina.paulus@ukr.de

17 Tel. +1-414-955-2511 Tel. +49-941-944-4640

18 Fax +1-414-955-6568 Fax +49-941-944-4641

19  
20 Abstract: 177 words

21 Text: 4,433 words

22  
23 Running Title: HCMV regulation of STAT3

24 **ABSTRACT**

25           In the canonical STAT3 signaling pathway, binding of agonist to receptors activates  
26 Janus kinases which phosphorylate cytoplasmic STAT3 at tyrosine 705 (Y705). Phosphorylated  
27 STAT3 dimers accumulate in the nucleus and drive the expression of genes involved in  
28 inflammation, angiogenesis, invasion and proliferation. Here we demonstrate that human  
29 cytomegalovirus (HCMV) infection rapidly promotes nuclear localization of STAT3 in the  
30 absence of robust phosphorylation at Y705. Furthermore, infection disrupts interleukin-6 (IL6)-  
31 induced phosphorylation of STAT3 and expression of a subset of IL6-induced STAT3-regulated  
32 genes including SOCS3. We show that the HCMV 72-kDa IE1 protein associates with STAT3  
33 and is necessary to localize STAT3 to the nucleus during infection. Furthermore, expression of  
34 IE1 is sufficient to disrupt IL6-induced phosphorylation of STAT3, binding of STAT3 to the  
35 SOCS3 promoter and SOCS3 gene expression. Finally, inhibition of STAT3 nuclear localization  
36 or STAT3 expression during infection is linked to diminished HCMV genome replication. Viral  
37 gene expression is also disrupted with the greatest impact seen following viral DNA synthesis.  
38 Our study identifies IE1 as a new regulator of STAT3 intracellular localization and IL6 signaling  
39 and points at an unanticipated role of STAT3 in HCMV infection.

40 **INTRODUCTION**

41 Human cytomegalovirus (HCMV) is a human herpesvirus that infects the majority of the  
42 world population. Primary exposure results in a lifelong infection. HCMV is an opportunistic  
43 pathogen that causes serious disease in immunocompromised patients and is a leading cause of  
44 congenital birth defects (41, 44). The current FDA-approved antiviral compounds inhibit viral  
45 DNA replication and have significantly improved the management of HCMV-associated  
46 diseases. Although the use of antivirals usually resolves viremia, the compounds fail to remove  
47 the latent reservoirs of HCMV within the body. Moreover, their use is limited due to toxicity,  
48 poor oral bioavailability and the selection of antiviral resistant variants (5, 20, 35). Efforts are  
49 underway to identify additional antiviral compounds to increase treatment options.

50 The 72-kDa immediate-early 1 (IE1) protein of HCMV is a key regulatory  
51 phosphoprotein conditionally required for viral early gene expression and replication in  
52 fibroblasts (18, 19, 42). IE1 localizes to the host cell nucleus, targeting both interchromatin  
53 compartments termed nuclear domain 10 (ND10) (2, 26, 68) and chromatin (29). Our work and a  
54 consecutive study by Huh et al. has demonstrated that IE1 forms physical complexes with  
55 STAT1 and STAT2 in the nuclei of infected cells, prevents association of STAT1, STAT2, and  
56 IRF9 with promoters of type I interferon (IFN)-stimulated genes and inhibits IFN- $\alpha$ -induced  
57 transcription (22, 27, 46). Consequently, IE1 disrupts type I IFN-dependent STAT signaling  
58 endowing the virus with partial resistance to the antiviral effects of IFN- $\alpha$  and IFN- $\beta$  (22, 27,  
59 46). Notably, this activity has been subsequently shown to be conserved across IE1 homologs of  
60 the human  $\beta$ -herpesvirus subfamily (23). Conversely, following ectopic expression in an  
61 inducible cell model (TetR/TetR-IE1), IE1 elicited a transcriptional response dominated by the  
62 up-regulation of pro-inflammatory and immune modulatory genes normally induced by IFN- $\gamma$

63 (25). Although IE1-mediated gene expression proved to be independent of IFN- $\gamma$ , it required the  
64 tyrosine-phosphorylated form of STAT1. Accordingly, STAT1 accumulated in the nucleus and  
65 became associated with IE1 target genes upon expression of the viral protein (25).

66 Another member of the STAT protein family, STAT3 is involved in regulating diverse  
67 responses. In total, four isoforms of STAT3 have been identified: full-length STAT3 $\alpha$  and  
68 truncated STAT3 $\beta$ , STAT3 $\gamma$ , and STAT3 $\delta$  (See review: 75). Although the function of the  
69 truncated isoforms is unclear, studies are beginning to suggest that they have distinct cellular  
70 activities from STAT3 $\alpha$  (37, 72, 76). STAT3 is activated by a variety of different stimuli  
71 including interleukin-6 (IL6) and other cytokines or growth factors (1, 75). In the canonical  
72 STAT3 signaling pathway, binding of agonist to receptors activates Janus kinases (JAKs) which  
73 phosphorylate cytoplasmic STAT3 at tyrosine 705 (Y705). Phosphorylated STAT3 dimers  
74 accumulate in the nucleus and drive the expression of genes involved in inflammation,  
75 angiogenesis, invasion and proliferation (1, 75). Nuclear translocation is mediated by the  
76 importin- $\alpha$  and  $\beta$ 1 heterodimer complex (9, 32). Furthermore, phosphorylation at serine 727  
77 (S727) is necessary for maximal STAT3 transcriptional activity (66, 67). Recent studies have  
78 demonstrated that STAT3 unphosphorylated at Y705 shuttles between the cytoplasm and the  
79 nucleus and is also transcriptionally active (48, 60, 70, 71).

80 In this study, we have determined a mechanism used by HCMV to regulate STAT3  
81 during infection. We demonstrate that HCMV IE1 is both necessary and sufficient to promote  
82 early nuclear localization of STAT3 which is predominately unphosphorylated at Y705. One  
83 functional consequence is the IE1-mediated disruption of STAT3-mediated IL6 signaling. In  
84 addition, inhibition of STAT3 nuclear localization was linked to reduced viral DNA replication  
85 and late gene expression.

## 86 MATERIALS AND METHODS

### 87 Biological Reagents

88 MRC-5 fibroblasts, ARPE-19 epithelial cells and U373 astrocytoma cells were  
89 propagated in Dulbecco's modified Eagle's medium supplemented with 7% fetal bovine serum  
90 (Life Technologies, Carlsbad, CA) and 1% penicillin/streptomycin (Life Technologies). Unless  
91 otherwise stated, cells were grown until confluent, serum starved in 0.5% fetal bovine serum for  
92 2 days and then infected at a multiplicity ranging from 0.25 to 5 infectious units per cell (IU/cell)  
93 in DMEM supplemented with 0.5% FBS. In several experiments, cells were treated 24 h prior to  
94 infection with the indicated inhibitors: 15  $\mu$ M curcumin (Sigma-Aldrich, St. Louis, MO), 30-150  
95  $\mu$ M S3i-201 (NSC 74859) (ThermoFisher Scientific, Waltham, MA), 5  $\mu$ M STATTIC (Santa  
96 Cruz), 4  $\mu$ M WP1066 (Santa Cruz) or DMSO (Sigma). Compounds were replaced every 24 h.  
97 As a control for pSTAT3 and STAT3-regulatable gene expression, U-373 cells were treated with  
98 183 ng/ml of carrier free recombinant human interleukin-6 (IL6) (BioLegend, San Diego, CA)  
99 for 15 min for Western blot analysis or 45 min for gene expression studies. Studies using MRC-5  
100 cells also included recombinant human IL6 receptor alpha (IL6R $\alpha$ ) (R&D Systems, Minneapolis,  
101 MN). TetR-IE1 and TetR cells have been previously described (25) and were treated with  
102 doxycycline (Dox) for 0 to 72 h at a final concentration of 1  $\mu$ g/ml. Viability and total cell  
103 numbers were determined with Viacount (EMD Millipore, Billerica, MA) and Gauva EasyCyte  
104 Mini Flow Cytometer (Millipore). Control siRNAs (Cell Signaling Technology), siRNA  
105 targeting importin- $\beta$ 1 (Life Technologies) or siRNA targeting STAT3 (On-TARGET-SMART  
106 pool) (ThermoFisher) were transfected using Lipofectamine 2000 (Life Technologies).

107 BAC-derived HCMV strains AD169 (AD $wt$ ) (73), AD $in27F$  (49) and Towne  $wt$  (36)  
108 were propagated in primary fibroblasts, and Towne  $dIIIE1$  virus (27) was propagated in TetR-IE1

109 cells. BAC-derived HCMV clinical virus TB40/E (54) was propagated in ARPE19 epithelial  
110 cells. Viral titers were determined by an infectious units assay (40) or standard plaque assay.

111

## 112 **Analysis of Protein, DNA, and Gene Expression**

113 Preparation of cell extracts, immunoprecipitation, Western blot analysis, and  
114 immunofluorescence microscopy were completed as previously described (27, 49, 59). The  
115 antibodies used are listed below. Immunofluorescence was observed using a 63× lens in a Leica  
116 DMRX inverted microscope (Leica Microsystems, Wetzlar, Germany) equipped with a Retiga-  
117 SRV digital camera and Image-Pro Plus 6.2 software (Q-Imaging, Surrey, Canada) (Figures 3, 5,  
118 and S2). Alternatively, a 60× lens in a Nikon Eclipse Ti-U inverted microscope (Nikon, Melville,  
119 NY) equipped with a CoolSNAP ES2 CCD camera (Photometrics), multichromatic Sedat Quad  
120 ET filter set (multichroic splitter, Chroma), and NIS-Elements software (Nikon) was used for  
121 image analysis (Figures 1, 2, 6, 8, and S1). The mean fluorescent intensity of STAT3 within the  
122 nucleus and cytoplasm was obtained from an average of 20-30 cells and from at least two  
123 replicate experiments unless otherwise noted. The data is presented as nuclear to cytoplasmic  
124 ratio  $\pm$  SEM. Viral DNA content and RNA expression from infected cells were determined using  
125 quantitative real-time PCR as previously described (27, 49) and primers listed below. Quantities  
126 for unknown samples were defined relative to an arbitrary standard curve consisting of 10-fold  
127 serial dilutions of one sample and completed for each primer pair. Chromatin  
128 immunoprecipitation (ChIP) coupled to qPCR was performed as described (25) using 10  $\mu$ g anti-  
129 STAT3 C-20 or normal rabbit IgG and primers specific to the human SOCS3 promoter or  
130 transcribed region (see below). For flow cytometry, U373 cells were dissociated from culture  
131 plates using enzyme-free cell dissociation buffer (Millipore). Cells were resuspended in PBS

132 with 2% BSA containing antibody-conjugate (Alexa Fluor 647) and incubated for 30 min at 4°C.  
133 Cells were washed three times using PBS with 2% BSA and then fixed with 2%  
134 paraformaldehyde. Data acquisition was performed on a BD LSR II and analyzed using FlowJo  
135 Software (Treestar, Ashland, OR).

136

### 137 **Antibodies**

138 The following antibodies were used in these studies: normal rabbit immunoglobulin G (IgG)  
139 (Sigma-Aldrich), mouse anti-FLAG M2 (Sigma-Aldrich), mouse anti-GAPDH clone 0411  
140 (Santa Cruz Biotechnology), rabbit anti-GAPDH ab9485 (Abcam), mouse anti-HA clone HA-7  
141 (Sigma-Aldrich), rabbit anti-STAT1 E-23 (Santa Cruz Biotechnology), rabbit anti-STAT2 H-190  
142 (Santa Cruz Biotechnology), mouse anti-STAT3 clone 124H6 (Cell Signaling Technology),  
143 rabbit anti-STAT3 C-20 (Santa Cruz Biotechnology), rabbit anti-pSTAT3 (Y705) (Cell  
144 Signaling Technology), rabbit anti-pSTAT3 (S727) (Cell Signaling Technology), rabbit anti-  
145 H2A ab15653 (Abcam), and rabbit anti-importin  $\beta$ 1 (Cell Signaling Technology). The antibodies  
146 against HCMV proteins were mouse anti-pUL123 clone 1B12, mouse anti-pUL122 clone 3A9,  
147 mouse anti-pTRS1, mouse anti-pUL99, mouse anti-pUL37 clone 2A1D, and mouse anti-pUL38  
148 clone 3D12 (generously provided by Dr. Tom Shenk, Princeton University) and mouse anti-  
149 pUL44 (Virusys). Secondary antibodies include goat anti-mouse HRP and donkey anti-rabbit  
150 HRP (Jackson ImmunoResearch) for Western blot analysis and anti-mouse Alexa Fluor 488,  
151 anti-mouse Alexa Fluor 568, anti-mouse Alexa Fluor 594, anti-rabbit Alexa Fluor 488 (Life  
152 Technologies), and Alexa Fluor 647 conjugated to anti-CD126 (IL-6R $\alpha$ ) (Biolegend, San Diego,  
153 CA) for immunofluorescence. Cellular DNA was stained with 4',6-diamidino-2-phenylindole  
154 (DAPI) (Life Technologies).

155

## 156 **PCR Oligonucleotides**

157 The following oligonucleotide pairs were used in these studies: IL6 (5'-  
158 AGCCACTCACCTCTTCAGAACGAA-3' and 5'-AGTGCCTCTTTGCTGCTTTCACAC-3'),  
159 SOCS3 (5'-ATTCGCCTTAAATGCTCCCTGTCC-3' and 5'-  
160 TGGCCAATACTTACTGGGCTGACA-3') and (5'-GGCCACTCTTCAGCATCTC-3' and 5'-  
161 ATCGTACTGGTCCAGGAACTC-3'), SOCS3 promoter (5'-AGCCTTTCTCTGCTGCGAGT-  
162 3' and 5'-CCCGATTCTGGAAGTGC-3'), TUBB (5'-TATCAGCAGTACCAGGAT GC-3'  
163 and 5'-TGAGAAGCCTGAGGTGATG-3'), GAPDH (5'-ACCCACTCCTCCACCTTTGAC-3'  
164 and 5'-CTGTTGCTGTAGCCAAATTCGT-3'), UL123 (5'-GCCTTCCCTAAGACCACCAAT -  
165 3' and 5'-ATTTTCTGGGCATAAGCCATAATC-3'), UL122 (5'-  
166 CCAGTATGCACCAGGTGTTAG-3' and 5'-CTGGATGCCCTTGTTGTTC-3'), UL38 (5'-  
167 ACGGTGCTATCGTGCTGGAGTATT-3' and 5'-AAGACCATCACCAGGTCGTCC ATA-3'),  
168 UL99 (5'-TTCACAAGGTCCACCCACC-3' and 5'-GTGTCCCATTCGACTCG-3'), and  
169 UL83 (5'-TGAGCATCTCAGGTAACCTGTTG-3' and 5'-CAGCCACGGGATCGTACTG-3').

170

## 171 **Statistical Analysis**

172 The data are representative of at least two independent experiments, and values are given  
173 as the mean of replicate experiments  $\pm$  standard error of the mean (SEM) unless otherwise stated.  
174 For all experiments using the Student's t-test, we have determined that the variances were not  
175 different using an F-test prior to using a t-test. A significant p value ( $p < 0.05$ ) is indicated by an  
176 asterisk in the figures.



177 **RESULTS**

178 **HCMV infection localizes unphosphorylated STAT3 to the nucleus and disrupts IL6-**

179 **induced gene expression.** Limited information is available on the impact of HCMV infection on

180 the cellular transcription factor STAT3. To determine whether HCMV influences STAT3, we

181 evaluated subcellular localization at 2 and 24 hpi. We infected U373 astrocytoma cells using

182 HCMV strain AD169 (ADwt) at a multiplicity of 5 infectious units (IU) per cell in 0.5% serum.

183 As a control, uninfected cells were treated with or without human IL6 to stimulate

184 phosphorylation of STAT3. Reduced serum conditions allowed for more robust IL6-stimulated

185 responses. Cells were fixed and stained using antibodies against STAT3 and phosphorylated

186 STAT3 (pSTAT3) at Y705. To quantify changes in localization, we determined the ratio of mean

187 fluorescent intensities between nuclear and cytosolic staining (N/C). We detected increased

188 STAT3 within the nuclei of infected cells at 2 hpi (N/C=2.95±0.05) and 24 hpi (N/C=6.71±0.68)

189 as compared to uninfected cells (N/C=1.25±0.16) (Figure 1A). As expected, we observed

190 increased nuclear localization of STAT3 (N/C=3.42±0.35) and pSTAT3 in mock plus IL6-

191 treated cells (Figure 1A). To our surprise, we detected little to no pSTAT3 within the nuclei of

192 infected cells (Figure 1A). These data suggest that HCMV infection rapidly promotes nuclear

193 localization of STAT3 in the absence of robust phosphorylation at Y705.

194 In general, phosphorylation of cytoplasmic STAT3 at Y705 occurs following cytokine

195 and growth factor stimulation and results in STAT3 nuclear accumulation and DNA binding (1,

196 75). We next investigated whether HCMV influences STAT3 phosphorylation during both

197 infection and cytokine stimulation. U373 cells were infected at an MOI of 5 IU/cell and cultures

198 were treated at the indicated times post infection with or without IL6 (Figure 1B). We evaluated

199 steady-state protein levels using Western blot analysis on whole cell lysates isolated from a

200 population of cells. Compared to mock infection treated with IL6, HCMV infection suppressed  
201 IL6-induced phosphorylation of STAT3 at Y705 by 2 hpi and continued through 48 hpi (Figure  
202 1B). In contrast, phosphorylation at S727 occurred regardless of infection and was independent  
203 of IL6 stimulation (Figure 1B). At a lower MOI, we observed increased STAT3 phosphorylation  
204 at Y705 by Western blot analysis which is likely occurring within uninfected cells in the  
205 population as determined by immunofluorescence analysis (Figure S1). To determine whether  
206 the response also occurs using a clinically relevant HCMV strain, we completed the experiment  
207 using the TB40/E virus (54). Similar to AD169, TB40/E infection suppressed IL6-induced  
208 phosphorylation at Y705 but not S727 (Figure 1C). These data demonstrate that HCMV infection  
209 disrupts IL6-induced phosphorylation of STAT3 at Y705.

210 We evaluated the impact of infection on the expression of two genes known to be  
211 regulated by STAT3, IL6 and SOCS3 (74, 75). We infected U373 cells at 1 IU/cell using AD*wt*  
212 virus with or without IL6 at the indicated times post infection and determined changes in gene  
213 expression using quantitative RT-PCR (qRT-PCR) relative to GAPDH RNA levels. Compared to  
214 mock control, infection significantly decreased gene expression of IL6 and SOCS3 following  
215 IL6 stimulation (Figure 1D). These data support the conclusion that HCMV infection disrupts  
216 expression of two IL6-induced STAT3-regulated genes. To exclude the possibility that  
217 disruption of IL6 signaling is a consequence of decreased IL6 receptor cell surface expression,  
218 we measured the impact of infection on IL6R $\alpha$ . We infected U373 cells at 3 IU/cell and surface  
219 levels of IL6R $\alpha$  were determined using flow cytometry. Compared to mock, we observed similar  
220 levels of IL6R $\alpha$  during HCMV infection at 6 and 24 hpi (Figure 1E). These data rule out the  
221 possibility of HCMV-mediated loss of endogenous IL6R $\alpha$  surface expression during the time of  
222 altered gene expression.

223 To test whether HCMV-mediated inhibition of IL6 signaling depends on STAT3 nuclear  
224 localization, we evaluated the effects on STAT3 phosphorylation after disruption of nuclear  
225 import. Nuclear translocation of STAT3 is mediated by the importin- $\alpha$  and  $\beta$ 1 heterodimer  
226 complex (9, 32). We transfected U373 cells with either a control siRNA or an siRNA targeting  
227 importin- $\beta$ 1 expression and observed a reduction in importin- $\beta$ 1 levels (Figure 2A). Under these  
228 conditions, reduced importin- $\beta$ 1 resulted in increased pSTAT3 in IL6-treated HCMV-infected  
229 cells (Figure 2A). Furthermore, disrupting importin- $\beta$ 1 reduced IL6-induced STAT3 nuclear  
230 accumulation in both mock (N/C=1.27 $\pm$ 0.11) and HCMV-infected cells (N/C=1.55 $\pm$ 0.12) as  
231 compared to control siRNA mock (N/C=2.19 $\pm$ 0.03) and infected (N/C=4.15 $\pm$ 0.10) (Figure 2B).  
232 These data suggest that HCMV is promoting nuclear accumulation of STAT3 early during  
233 infection thereby moving STAT3 away from the cytosolic regulators.

234 Changes in STAT3 phosphorylation and localization are detectable as early as 2 hpi  
235 indicating a role for HCMV virions or newly expressed proteins in manipulating STAT3. To  
236 identify the source of the activity, U373 cells were infected with either untreated AD $_{wt}$  or UV-  
237 irradiated virus and evaluated by immunofluorescence microscopy. STAT3 nuclear localization  
238 occurred following infection with untreated (N/C=3.27 $\pm$ 0.15) but not UV-irradiated virus  
239 (N/C=1.09 $\pm$ 0.02) (Figure 2C). Under these conditions of UV treatment, we did not detect IE1  
240 RNA expression (Figure 2D). These data demonstrate that viral gene expression is necessary for  
241 relocalization of STAT3.

242

243 **HCMV IE1 promotes STAT3 nuclear accumulation and disrupts IL6-induced STAT3**

244 **phosphorylation, DNA binding and target gene expression.**

245 HCMV immediate early protein IE1 is known to regulate both STAT1 and STAT2 (22,  
246 25, 27, 46). To determine whether IE1 expression could influence STAT3 localization, MRC-5  
247 fibroblasts were mock-infected or infected with either wild-type (*wt*) or an IE1-deficient virus  
248 (*dIE1*) of the HCMV Towne strain at 3 PFU/cell. Using immunofluorescence microscopy, we  
249 observed increased staining of STAT3 within the nuclei of IE2-positive infected cells by 6 hpi  
250 using *wt* virus (N/C=1.73±0.04) but not *dIE1* (N/C=0.99±0.15) as compared to mock  
251 (N/C=1.09±0.13) (Figure 3A). This increase was also observed at both 24 (N/C=1.73±0.55) and  
252 72 hpi (N/C=2.13±0.56) (Figure 3A). At these later times, we did observe a few cells in the  
253 *dIE1* infections that had increased nuclear STAT3 staining; however, this was not significant  
254 among the population as indicated by the N/C ratio determined from a random selection of cells  
255 (n=95). These data demonstrate that IE1 is necessary for the efficient nuclear localization of  
256 STAT3 during infection. HCMV IE1 has been previously demonstrated to localize to mitotic  
257 chromatin (27). In cells undergoing mitosis in the infected population, we observed  
258 colocalization of STAT3 with DAPI-stained chromatin (Figure 3B, left and right panel).  
259 Moreover, STAT3 and IE1 colocalized in *wt*- but not *dIE1*-infected cells (Figure 3B, right  
260 panel). To assess a possible physical interaction between IE1 and STAT3, we isolated whole cell  
261 lysates at 24 hpi and immunoprecipitated protein complexes using an antibody against IE1.  
262 Following immunoprecipitation, we detected the slower migrating STAT3 $\alpha$  but not the smaller  
263 STAT3 isoform by Western blot analysis from TN*wt*-infected cells (Figure 3C). We did not  
264 observe an interaction when using an antibody against IE2 or following infection by the *dIE1*  
265 virus (Figure 3C). IE1 was also specifically detected throughout the viral infectious cycle (6 to  
266 72 h) in protein complexes isolated by immunoprecipitation using a STAT3-directed antibody

267 (Figure 3D). These data demonstrate that HCMV IE1 associates with at least one STAT3  
268 isoform during infection.

269 Finally, we evaluated the functional impact of IE1 on STAT3 following IL6 stimulation.  
270 These studies were completed by adding both IL6 and soluble IL6 receptor alpha (IL6R $\alpha$ ) to the  
271 culture media, because MRC-5 cells are largely unresponsive to IL6 alone. Following the  
272 addition of exogenous IL6/IL6R $\alpha$ , infection by *wt* but not *dIE1* virus resulted in reduced levels  
273 of Y705-phosphorylated STAT3 at 16 hpi as compared to mock (Figure 4A). Under these  
274 conditions in mock infected cells, IL6/IL6R $\alpha$  triggered robust STAT3 DNA binding at the  
275 SOCS3 promoter and little binding at the SOCS3 transcribed region, as determined by chromatin  
276 immunoprecipitation (ChIP) assay (Figure 4B). During infection, IL6/IL6R $\alpha$ -induced STAT3  
277 DNA binding was substantially diminished using *wt* virus but not the *dIE1* virus (Figure 4B).  
278 Concordantly, SOCS3 gene induction was significantly reduced during *wt* infection (Figure 4C).  
279 Infection by the *dIE1* virus altered SOCS3 expression, but to a lesser degree than *wt* virus  
280 (Figure 4C). Expression of HCMV IE2 was unaltered between the different conditions of  
281 infection (Figure 4C). Our results support the conclusion that HCMV IE1 binds to STAT3 $\alpha$  and  
282 is necessary to localize STAT3 to the nucleus at early times of infection. Furthermore,  
283 expression of IE1 disrupts IL6-induced phosphorylation of STAT3, DNA association by STAT3,  
284 and SOCS3 gene induction during infection.

285 To determine whether IE1 expression is sufficient to mediate these changes, we induced  
286 IE1 in the absence of infection using a tetracycline repressor-regulated expression system in  
287 human fibroblasts (TetR/TetR-IE1) (25). Following induction of IE1 expression using  
288 doxycycline, we observed strong accumulation of STAT3 within the nuclei of TetR-IE1 cells  
289 (Figure 5A). STAT3 relocalization did not occur in control TetR cells (Figure 5A). By 24 to 72 h

290 post stimulation, greater than 90% of the IE1-positive cells contained STAT3 within the nucleus  
291 (Figure 5B), but these nuclei did not exhibit detectable pSTAT3 (Figure S3). Furthermore,  
292 STAT3 again colocalized with the viral protein and DAPI-stained mitotic chromatin upon  
293 induction of IE1 (Figure 5C). Consistent with previous studies (25), induction of IE1 expression  
294 relocalized only a fraction of STAT1 to the nucleus with delayed kinetics as compared to STAT3  
295 (Figure S2A and C) while not apparently altering the subcellular distribution of STAT2 (Figure  
296 S2B and C). We also evaluated changes in STAT3 phosphorylation upon IE1 expression.  
297 Increased expression of IE1 correlated with decreased levels of phosphorylation at Y705, while  
298 the total levels of STAT3 remained constant (Figure 5D). Under these conditions, IE1 was  
299 sufficient to suppress the levels of SOCS3 RNA (Figure 5E). Finally, induction of IE1  
300 suppressed exogenous IL6/IL6R $\alpha$ -stimulated phosphorylation of STAT3 (Figure 5F and S3),  
301 SOCS3 promoter binding by STAT3 (Figure 5G) and SOCS3 expression (Figure 5H). These data  
302 indicate that expression of IE1 is sufficient to promote the nuclear accumulation of mostly  
303 unphosphorylated STAT3 inactive for sequence-specific DNA binding at the SOCS3 promoter  
304 and alter expression of the STAT3-regulated gene SOCS3.

305

306 **Disruption of STAT3 relocalization inhibits HCMV DNA replication.** The rapid  
307 accumulation of unphosphorylated STAT3 in the nucleus during infection suggests that HCMV  
308 might utilize STAT3 for viral replication. To test this hypothesis, we evaluated the impact of  
309 chemical inhibitors of STAT3 on HCMV infection. The inhibitors included S3i-201 which  
310 inhibits STAT3 dimerization and DNA binding (53), curcumin, a natural plant polyphenol which  
311 functions, in part, by inhibiting STAT3 DNA binding (3, 7, 15, 28), STATTIC which interferes  
312 with STAT3 phosphorylation and dimerization (51), and WP1066 which blocks upstream JAK2-

313 mediated phosphorylation (14). Initially, we tested whether the compounds would influence  
314 HCMV-mediated localization of STAT3. U373 cells were pretreated with DMSO or non-  
315 cytotoxic concentrations of each compound (Figure 6A). We infected cells at a multiplicity of 5  
316 IU/cell and evaluated STAT3 by immunofluorescence microscopy. Compared to DMSO  
317 (N/C=5.30±0.12), both S3i-201 (N/C=1.26±0.10) and curcumin (N/C=1.13±0.40) treatments  
318 significantly reduced the accumulation of STAT3 in the nucleus of infected cells (Figure 6B).  
319 STATTC treatment resulted in an intermediate phenotype (N/C=2.64±0.80) while inhibiting  
320 JAK-mediated phosphorylation using WP1066 failed to block the HCMV-mediated change in  
321 STAT3 localization (N/C=5.45±0.90) (Figure 6B).

322         Next, we quantified the impact of inhibiting STAT3 on HCMV replication. U373 cells  
323 were pretreated with DMSO or compound and infected at 0.25 IU/cell using AD*wt* virus. We  
324 quantified changes in HCMV viral DNA levels using qPCR. The addition of S3i-201 resulted in  
325 a 99.7% reduction in viral DNA levels, curcumin in a 94.0% reduction, STATTC in an 89.5%  
326 reduction and WP1066 had no effect on DNA replication (Figure 6C). Interestingly, the percent  
327 reduction was proportional to the change in the nuclear/cytosolic ratio for STAT3 (Figure 6B).  
328 Using S3i-201, we observed the greatest decrease in DNA replication at ≥120 μM (Figure 7A).  
329 The efficacy of S3i-201 inhibition was influenced by MOI. Although still inhibiting replication,  
330 infection at 3 IU/cell resulted in approximately 71.2 % decrease in viral DNA replication (Figure  
331 7B). We also evaluated the antiviral efficacy of S3i-201 during infection of primary human  
332 foreskin fibroblasts and retinal pigmented epithelial cells. Fibroblasts and U373 cells were  
333 infected at 0.25 IU/cell using AD*wt* virus while epithelial cells were infected using the clinical  
334 isolate TB40/E. Chemical inhibition of STAT3 significantly reduced viral DNA replication at 72  
335 hpi in all of the cell types and viral strains (Figure 7C). Finally, we determined the impact of

336 STAT3 inhibition on viral titers at 96 hpi from cells treated with either DMSO or S3i-201. We  
337 observed that the addition of S3i-201 resulted in an average 2.3 log reduction in viral titers  
338 (Figure 7D). These data suggest that STAT3 nuclear localization is linked to efficient HCMV  
339 DNA replication and virus production in multiple cell types.

340 To provide evidence that the disruption is STAT3-dependent, we knocked-down STAT3  
341 expression by transfecting U373 cells with an siRNA targeting STAT3 or control siRNA. We  
342 analyzed changes in STAT3 protein expression by Western blot and observed a reduction in  
343 STAT3 levels using the specific siRNA as compared to control (Figure 8A). Albeit reduced, we  
344 did observe STAT3 within the nucleus in cells transfected with the specific siRNA (Figure 8B).  
345 To evaluate the impact on HCMV viral DNA replication, siRNA-transfected U373 cells were  
346 infected a 0.25 IU/cell and we quantified changes in viral DNA levels using qPCR. Compared to  
347 control, we observed a 5-fold reduction in viral DNA replication upon reduced levels of STAT3  
348 (Figure 8C). These data provide additional evidence that STAT3 is necessary for fully efficient  
349 viral DNA replication.

350 Herpesvirus gene expression is temporally regulated with kinetic classes defined as  
351 immediate early (IE), early (E), early-late (E-L) and late (L). Efficient late gene expression is  
352 dependent upon DNA replication (41). To identify the steps in replication which require STAT3,  
353 we quantified changes in viral gene expression. U373 cells were pretreated with DMSO or S3i-  
354 201 and infected using AD<sub>wt</sub> virus at 0.25 IU/cell. Total RNA was harvested and viral gene  
355 expression was quantified relative to GAPDH RNA. We observed similar levels of expression  
356 for the IE and E genes UL123 (IE1) and UL38, respectively, between mock and S3i-201  
357 treatments (Figure 9A). However, beginning around 24 hpi, the addition of S3i-201 significantly  
358 decreased expression of UL122 (IE2), UL83, and UL99 (Figure 9A). We confirmed these



359 changes using Western blot analysis of whole cell lysates from HCMV-infected U373 cells  
360 (Figure 9B). In addition to changes in the IE2-86 kDa (pUL122) protein, we observed decreased  
361 expression of the IE2-60 kDa late isoform following S3i-201 treatment (Figure 9B).  
362 Furthermore, expression levels of two viral proteins with E-L kinetics, pTRS1 and pUL44, were  
363 also inhibited (Figure 9B) beginning at 24 hpi. These data demonstrate that inhibition of STAT3  
364 disrupts viral gene expression beginning around 24 hpi with the greatest impact seen after 48 hpi  
365 on HCMV IE2, E-L and L genes.

366         The accumulation of E-L and L transcripts as well as UL122 is dependent on viral DNA  
367 synthesis (12, 57, 58). Furthermore, HCMV IE2, pUL44, and pTRS1 have been demonstrated to  
368 contribute to genome replication (21, 33, 34, 36, 50, 56, 65). To test the timing of STAT3's  
369 contribution to HCMV replication, we treated U373 cells with S3i-201 at different times during  
370 infection. Cells were infected at 0.25 IU/cell using AD*wt* virus and treated with S3i-201 at 2 hpi  
371 or at 48 hpi for 24 h. We isolated DNA at 72 hpi and quantified viral genomes using qPCR.  
372 Consistent with previous data, S3i-201 treatment early during infection resulted in a significant  
373 decrease in viral DNA levels (Figure 9C). Conversely, treatment at 48 hpi resulted in no  
374 significant difference in viral DNA compared to control infection (Figure 9C). These data  
375 suggest that HCMV relocalizes STAT3 early to regulate early and late events during infection,  
376 including efficient viral DNA replication.

377

## 378 **DISCUSSION**

379         We have determined that HCMV infection promotes the nuclear accumulation of STAT3  
380 that is predominantly or entirely unphosphorylated at tyrosine 705 (Y705). In the canonical  
381 pathway from uninfected cells, STAT3 is activated by a variety of different stimuli including

382 cytokines and growth factors, resulting in phosphorylation of Y705 (pSTAT3) and accumulation  
383 in the nucleus (1, 75). Unlike HCMV, herpesviruses that infect cells of lymphoid origin  
384 including Epstein-Barr virus (EBV) (17, 64), Kaposi's sarcoma-associated herpesvirus (KSHV)  
385 (47), herpesvirus saimiri (HVS) (8), and varicella-zoster virus (VZV) (52) exploit the survival  
386 and oncogenic effects of pSTAT3. Beyond herpesviruses, several oncogenic viruses utilize  
387 pSTAT3 while other viruses employ mechanisms to inhibit STAT3 signaling (62, 63). Within  
388 our studies, we observed that disrupting the nuclear accumulation of STAT3 or STAT3  
389 expression inhibited HCMV infection at the stage of viral DNA replication. These studies are the  
390 first example of a virus that inhibits phosphorylation of STAT3 at Y705 yet still requires its  
391 activities for viral replication.

392         We have demonstrated that the HCMV IE1 protein is necessary to relocalize STAT3 to  
393 the nucleus at early times during infection, and the viral protein is also sufficient to induce  
394 nuclear STAT3 accumulation. The effects of IE1 on the subcellular distribution of STAT3 seem  
395 to be independent of phosphorylation at Y705 or cytokine stimulation. IE1 (also known as IE1-  
396 72kDa or IE72) is a nuclear regulatory phosphoprotein expressed from the HCMV genome at the  
397 start of infection. IE1 has long been known to attach to human chromosomes (29), but is not  
398 considered to bind directly to DNA (43). We observed that IE1 expression promotes the  
399 association of STAT3 with mitotic chromatin yet disrupts STAT3 binding to the SOCS3  
400 promoter. Unphosphorylated STAT3 has been demonstrated to shuttle between the nucleus and  
401 the cytosol (48, 60, 70, 71), and we speculate that STAT3 nuclear export may be prevented by  
402 interactions with IE1 at cellular chromatin and/or other nuclear compartments.

403         One functional consequence of IE1-mediated nuclear localization of STAT3 is the  
404 suppression of IL6-induced SOCS3 gene expression. When disrupting nuclear import, we were

405 able to re-establish IL6-stimulated phosphorylation of STAT3 suggesting that HCMV is  
406 sequestering STAT3 away from its upstream kinases by nuclear localization. In addition,  
407 disruption of JAK signaling using the compound WP1066 failed to prevent HCMV-mediated  
408 nuclear localization or disrupt viral DNA replication. However, we cannot exclude the possibility  
409 of HCMV modulation of regulatory phosphatases. Previous studies have demonstrated that up-  
410 regulation of IL6 by HCMV pUS28 resulted in pSTAT3 at Y705 (55). Consistent with these and  
411 other studies (11, 55), we observed a transient increase in IL6 expression occurring only at 2 hpi  
412 which was not affected by S3i-201 (data not shown). Furthermore, we did detect increased  
413 pSTAT3 (Y705) by Western blot when infecting most but not all of the cells in culture. Under  
414 these conditions, phosphorylation of STAT3 occurred mostly in the uninfected cells within this  
415 population. Finally, Le et al. (30) have demonstrated that HCMV infection can disrupt IFN- $\gamma$ -  
416 stimulated STAT3 phosphorylation starting at 24 hpi. Our studies indicate that nuclear STAT3 is  
417 predominantly unphosphorylated at Y705 in cells infected by either lab-adapted or clinical  
418 strains of HCMV.

419 Our data indicates that HCMV primarily utilizes unphosphorylated STAT3 to promote,  
420 either directly or indirectly, the initiation of HCMV DNA replication. Consistent with this idea,  
421 the addition of S3i-201 after 48 hpi had no effect on DNA replication. We have demonstrated  
422 that inhibition of STAT3 severely attenuates viral DNA replication, the expression of numerous  
423 viral genes, and consequently, the production of infectious viral progeny. At 24 hpi, we observed  
424 similar levels of expression for HCMV IE1, IE2 and pUL38 following STAT3 inhibition.  
425 However, we detected a substantial decrease in expression of the viral polymerase subunit,  
426 pUL44. The decrease in pUL44 levels may be attributed to decreased pTRS1 since pTRS1  
427 functions in cooperation with IE1 and IE2 to stimulate UL44 expression (10, 56). After 24 hpi,

428 the increase in IE2-86kDa, IE2-60kDa, pTRS1 and pUL99 levels failed to occur upon inhibiting  
429 STAT3. These changes have been shown to be dependent upon viral DNA replication (4, 13, 38,  
430 45). A similar phenotype occurred upon deletion of the HCMV protein pUL21a which, along  
431 with pUL97 kinase, negatively regulates the anaphase promoting complex (12, 13, 61).  
432 Disruption of pUL21a resulted in reduced DNA replication and late expression of a subset of  
433 proteins including IE2 and pUL99 (13).

434 We have demonstrated that chemical antagonists of STAT3 significantly inhibit HCMV  
435 infection. Similar observations have been made using inhibitors of STAT3 and VZV infection  
436 (52). Numerous malignancies are characterized by elevated STAT3 expression and activity (24).  
437 As a result, STAT3 inhibitors are being developed and are currently entering clinical trials as  
438 anti-cancer agents (24). Several FDA-approved compounds have been shown to inhibit STAT3  
439 activity, such as Celebrex and Sorafenib (16, 31, 69), which also inhibit HCMV replication *in*  
440 *vitro* (6, 39). Overall, our studies indicate that HCMV manipulates STAT3 to promote an  
441 environment that supports efficient viral DNA replication and implicate STAT3 as a possible  
442 target of anti-HCMV antiviral research.

443

#### 444 **ACKNOWLEDGEMENT**

445 We thank T. Shenk for the HCMV antibodies. We thank Theresa Knoblach, Benedikt  
446 Grandel, Nathalie Czech, and Thomas Harwardt for experimental contributions and Sandra  
447 Meinel for technical assistance. We also thank M. Hakki and the members of the Terhune and  
448 Nevels labs for their insights and helpful discussions.

449 This work is supported by NIH grant R01AI083281 to S. Terhune and by Deutsche  
450 Forschungsgemeinschaft grant PA851/2-1 to C. Paulus.

451 **REFERENCES**

- 452 1. **Aggarwal, B. B., A. B. Kunnammakara, K. B. Harikumar, S. R. Gupta, S. T.**  
453 **Tharakan, C. Koca, S. Dey, and B. Sung.** 2009. Signal transducer and activator of  
454 transcription-3, inflammation, and cancer: how intimate is the relationship? *Ann N Y*  
455 *Acad Sci* **1171**:59-76.
- 456 2. **Ahn, J. H., and G. S. Hayward.** 1997. The major immediate-early proteins IE1 and IE2  
457 of human cytomegalovirus colocalize with and disrupt PML-associated nuclear bodies at  
458 very early times in infected permissive cells. *J Virol* **71**:4599-4613.
- 459 3. **Alexandrow, M. G., L. J. Song, S. Altiok, J. Gray, E. B. Haura, and N. B. Kumar.**  
460 2012. Curcumin: a novel Stat3 pathway inhibitor for chemoprevention of lung cancer.  
461 *Eur J Cancer Prev* **21**:407-412.
- 462 4. **Alvarez-Castelao, B., I. Martin-Guerrero, A. Garcia-Orad, and J. G. Castano.** 2009.  
463 Cytomegalovirus promoter up-regulation is the major cause of increased protein levels of  
464 unstable reporter proteins after treatment of living cells with proteasome inhibitors. *J Biol*  
465 *Chem* **284**:28253-28262.
- 466 5. **Avery, R. K.** 2008. Update in management of ganciclovir-resistant cytomegalovirus  
467 infection. *Curr Opin Infect Dis* **21**:433-437.
- 468 6. **Baryawno, N., A. Rahbar, N. Wolmer-Solberg, C. Taher, J. Odeberg, A. Darabi, Z.**  
469 **Khan, B. Sveinbjornsson, O. M. FuskevAg, L. Segerstrom, M. Nordenskjold, P.**  
470 **Siesjo, P. Kogner, J. I. Johnsen, and C. Soderberg-Naucler.** 2011. Detection of human  
471 cytomegalovirus in medulloblastomas reveals a potential therapeutic target. *J Clin Invest*  
472 **121**:4043-4055.

- 473 7. **Bill, M. A., J. R. Fuchs, C. Li, J. Yui, C. Bakan, D. M. Benson, Jr., E. B. Schwartz,**  
474 **D. Abdelhamid, J. Lin, D. G. Hoyt, S. L. Fossey, G. S. Young, W. E. Carson, 3rd, P.**  
475 **K. Li, and G. B. Lesinski.** 2010. The small molecule curcumin analog FLLL32 induces  
476 apoptosis in melanoma cells via STAT3 inhibition and retains the cellular response to  
477 cytokines with anti-tumor activity. *Mol Cancer* **9**:165.
- 478 8. **Chung, Y. H., N. H. Cho, M. I. Garcia, S. H. Lee, P. Feng, and J. U. Jung.** 2004.  
479 Activation of Stat3 transcription factor by Herpesvirus saimiri STP-A oncoprotein. *J*  
480 *Virol* **78**:6489-6497.
- 481 9. **Cimica, V., H. C. Chen, J. K. Iyer, and N. C. Reich.** 2011. Dynamics of the STAT3  
482 transcription factor: nuclear import dependent on Ran and importin-beta1. *PLoS One*  
483 **6**:e20188.
- 484 10. **Colberg-Poley, A. M.** 1996. Functional roles of immediate early proteins encoded by the  
485 human cytomegalovirus UL36-38, UL115-119, TRS1/IRS1 and US3 loci. *Intervirology*  
486 **39**:350-360.
- 487 11. **Dumortier, J., D. N. Streblov, A. V. Moses, J. M. Jacobs, C. N. Kreklywich, D.**  
488 **Camp, R. D. Smith, S. L. Orloff, and J. A. Nelson.** 2008. Human cytomegalovirus  
489 secretome contains factors that induce angiogenesis and wound healing. *J Virol* **82**:6524-  
490 6535.
- 491 12. **Fehr, A. R., N. C. Gualberto, J. P. Savaryn, S. S. Terhune, and D. Yu.** 2012.  
492 Proteasome-dependent disruption of the E3 ubiquitin ligase anaphase-promoting complex  
493 by HCMV protein pUL21a. *PLoS Pathog* **8**:e1002789.

- 494 13. **Fehr, A. R., and D. Yu.** 2011. Human cytomegalovirus early protein pUL21a promotes  
495 efficient viral DNA synthesis and the late accumulation of immediate-early transcripts. *J*  
496 *Virol* **85**:663-674.
- 497 14. **Ferrajoli, A., S. Faderl, Q. Van, P. Koch, D. Harris, Z. Liu, I. Hazan-Halevy, Y.**  
498 **Wang, H. M. Kantarjian, W. Priebe, and Z. Estrov.** 2007. WP1066 disrupts Janus  
499 kinase-2 and induces caspase-dependent apoptosis in acute myelogenous leukemia cells.  
500 *Cancer Res* **67**:11291-11299.
- 501 15. **Fossey, S. L., M. D. Bear, J. Lin, C. Li, E. B. Schwartz, P. K. Li, J. R. Fuchs, J.**  
502 **Fenger, W. C. Kisseberth, and C. A. London.** 2011. The novel curcumin analog  
503 FLLL32 decreases STAT3 DNA binding activity and expression, and induces apoptosis  
504 in osteosarcoma cell lines. *BMC Cancer* **11**:112.
- 505 16. **Ghosh, N., R. Chaki, V. Mandal, and S. C. Mandal.** 2010. COX-2 as a target for  
506 cancer chemotherapy. *Pharmacol Rep* **62**:233-244.
- 507 17. **Gires, O., F. Kohlhuber, E. Kilger, M. Baumann, A. Kieser, C. Kaiser, R. Zeidler, B.**  
508 **Scheffer, M. Ueffing, and W. Hammerschmidt.** 1999. Latent membrane protein 1 of  
509 Epstein-Barr virus interacts with JAK3 and activates STAT proteins. *EMBO J* **18**:3064-  
510 3073.
- 511 18. **Greaves, R. F., J. M. Brown, J. Vieira, and E. S. Mocarski.** 1995. Selectable insertion  
512 and deletion mutagenesis of the human cytomegalovirus genome using the *Escherichia*  
513 *coli* guanosine phosphoribosyl transferase (*gpt*) gene. *J Gen Virol* **76 ( Pt 9)**:2151-2160.
- 514 19. **Greaves, R. F., and E. S. Mocarski.** 1998. Defective growth correlates with reduced  
515 accumulation of a viral DNA replication protein after low-multiplicity infection by a  
516 human cytomegalovirus *ie1* mutant. *J Virol* **72**:366-379.

- 517 20. **Hakki, M., and S. Chou.** 2011. The biology of cytomegalovirus drug resistance. *Curr*  
518 *Opin Infect Dis* **24**:605-611.
- 519 21. **Heider, J. A., W. A. Bresnahan, and T. E. Shenk.** 2002. Construction of a rationally  
520 designed human cytomegalovirus variant encoding a temperature-sensitive immediate-  
521 early 2 protein. *Proc Natl Acad Sci U S A* **99**:3141-3146.
- 522 22. **Huh, Y. H., Y. E. Kim, E. T. Kim, J. J. Park, M. J. Song, H. Zhu, G. S. Hayward,**  
523 **and J. H. Ahn.** 2008. Binding STAT2 by the acidic domain of human cytomegalovirus  
524 IE1 promotes viral growth and is negatively regulated by SUMO. *J Virol* **82**:10444-  
525 10454.
- 526 23. **Jaworska, J., A. Gravel, and L. Flamand.** 2010. Divergent susceptibilities of human  
527 herpesvirus 6 variants to type I interferons. *Proc Natl Acad Sci U S A* **107**:8369-8374.
- 528 24. **Johnston, P. A., and J. R. Grandis.** 2011. STAT3 signaling: anticancer strategies and  
529 challenges. *Mol Interv* **11**:18-26.
- 530 25. **Knobloch, T., B. Grandel, J. Seiler, M. Nevels, and C. Paulus.** 2011. Human  
531 cytomegalovirus IE1 protein elicits a type II interferon-like host cell response that  
532 depends on activated STAT1 but not interferon-gamma. *PLoS Pathog* **7**:e1002016.
- 533 26. **Koriath, F., G. G. Maul, B. Plachter, T. Stamminger, and J. Frey.** 1996. The nuclear  
534 domain 10 (ND10) is disrupted by the human cytomegalovirus gene product IE1. *Exp*  
535 *Cell Res* **229**:155-158.
- 536 27. **Krauss, S., J. Kaps, N. Czech, C. Paulus, and M. Nevels.** 2009. Physical requirements  
537 and functional consequences of complex formation between the cytomegalovirus IE1  
538 protein and human STAT2. *J Virol* **83**:12854-12870.



- 539 28. **Kumar, A., and Bora, U.** 2012. Molecular docking studies on inhibition of Stat3  
540 dimerization by curcumin natural derivatives and its conjugates with amino acids.  
541 *Bioinformation* **8**:988-993.
- 542 29. **Lafemina, R. L., M. C. Pizzorno, J. D. Mosca, and G. S. Hayward.** 1989. Expression  
543 of the acidic nuclear immediate-early protein (IE1) of human cytomegalovirus in stable  
544 cell lines and its preferential association with metaphase chromosomes. *Virology*  
545 **172**:584-600.
- 546 30. **Le, V. T., M. Trilling, M. Wilborn, H. Hengel, and A. Zimmermann.** 2008. Human  
547 cytomegalovirus interferes with signal transducer and activator of transcription (STAT) 2  
548 protein stability and tyrosine phosphorylation. *J Gen Virol* **89**:2416-2426.
- 549 31. **Liu, D. B., G. Y. Hu, G. X. Long, H. Qiu, Q. Mei, and G. Q. Hu.** 2012. Celecoxib  
550 induces apoptosis and cell-cycle arrest in nasopharyngeal carcinoma cell lines via  
551 inhibition of STAT3 phosphorylation. *Acta Pharmacol Sin* **33**:682-690.
- 552 32. **Liu, L., K. M. McBride, and N. C. Reich.** 2005. STAT3 nuclear import is independent  
553 of tyrosine phosphorylation and mediated by importin-alpha3. *Proc Natl Acad Sci U S A*  
554 **102**:8150-8155.
- 555 33. **Loregian, A., B. A. Appleton, J. M. Hogle, and D. M. Coen.** 2004. Residues of human  
556 cytomegalovirus DNA polymerase catalytic subunit UL54 that are necessary and  
557 sufficient for interaction with the accessory protein UL44. *J Virol* **78**:158-167.
- 558 34. **Loregian, A., B. A. Appleton, J. M. Hogle, and D. M. Coen.** 2004. Specific residues in  
559 the connector loop of the human cytomegalovirus DNA polymerase accessory protein  
560 UL44 are crucial for interaction with the UL54 catalytic subunit. *J Virol* **78**:9084-9092.

- 561 35. **Lurain, N. S., and S. Chou.** 2010. Antiviral drug resistance of human cytomegalovirus.  
562 Clin Microbiol Rev **23**:689-712.
- 563 36. **Marchini, A., H. Liu, and H. Zhu.** 2001. Human cytomegalovirus with IE-2 (UL122)  
564 deleted fails to express early lytic genes. J Virol **75**:1870-1878.
- 565 37. **Maritano, D., M. L. Sugrue, S. Tininini, S. Dewilde, B. Strobl, X. Fu, V. Murray-**  
566 **Tait, R. Chiarle, and V. Poli.** 2004. The STAT3 isoforms alpha and beta have unique  
567 and specific functions. Nature immunology **5**:401-409.
- 568 38. **Marshall, E. E., C. J. Bierle, W. Brune, and A. P. Geballe.** 2009. Essential role for  
569 either TRS1 or IRS1 in human cytomegalovirus replication. J Virol **83**:4112-4120.
- 570 39. **Michaelis, M., C. Paulus, N. Loschmann, S. Dauth, E. Stange, H. W. Doerr, M.**  
571 **Nevels, and J. Cinatl, Jr.** 2011. The multi-targeted kinase inhibitor sorafenib inhibits  
572 human cytomegalovirus replication. Cell Mol Life Sci **68**:1079-1090.
- 573 40. **Mitchell, D. P., J. P. Savaryn, N. J. Moorman, T. Shenk, and S. S. Terhune.** 2009.  
574 Human cytomegalovirus UL28 and UL29 open reading frames encode a spliced mRNA  
575 and stimulate accumulation of immediate-early RNAs. J Virol **83**:10187-10197.
- 576 41. **Mocarski, E., Shenk, T., and Pass, R.F. .** 2007. Cytomegalovirus, vol. 5. Lippincott  
577 Williams & Wilkins, Philadelphia.
- 578 42. **Mocarski, E. S., G. W. Kemble, J. M. Lyle, and R. F. Greaves.** 1996. A deletion  
579 mutant in the human cytomegalovirus gene encoding IE1(491aa) is replication defective  
580 due to a failure in autoregulation. Proc Natl Acad Sci U S A **93**:11321-11326.
- 581 43. **Munch, K., M. Messerle, B. Plachter, and U. H. Koszinowski.** 1992. An acidic region  
582 of the 89K murine cytomegalovirus immediate early protein interacts with DNA. J Gen  
583 Virol **73 ( Pt 3)**:499-506.

- 584 44. **Nassetta, L., D. Kimberlin, and R. Whitley.** 2009. Treatment of congenital  
585 cytomegalovirus infection: implications for future therapeutic strategies. *J Antimicrob*  
586 *Chemother* **63**:862-867.
- 587 45. **Nevels, M., W. Brune, and T. Shenk.** 2004. SUMOylation of the human  
588 cytomegalovirus 72-kilodalton IE1 protein facilitates expression of the 86-kilodalton IE2  
589 protein and promotes viral replication. *J Virol* **78**:7803-7812.
- 590 46. **Paulus, C., S. Krauss, and M. Nevels.** 2006. A human cytomegalovirus antagonist of  
591 type I IFN-dependent signal transducer and activator of transcription signaling. *Proc Natl*  
592 *Acad Sci U S A* **103**:3840-3845.
- 593 47. **Punjabi, A. S., P. A. Carroll, L. Chen, and M. Lagunoff.** 2007. Persistent activation of  
594 STAT3 by latent Kaposi's sarcoma-associated herpesvirus infection of endothelial cells. *J*  
595 *Virol* **81**:2449-2458.
- 596 48. **Reich, N. C., and L. Liu.** 2006. Tracking STAT nuclear traffic. *Nat Rev Immunol*  
597 **6**:602-612.
- 598 49. **Reitsma, J. M., J. P. Savaryn, K. Faust, H. Sato, B. D. Halligan, and S. S. Terhune.**  
599 2011. Antiviral inhibition targeting the HCMV kinase pUL97 requires pUL27-dependent  
600 degradation of Tip60 acetyltransferase and cell-cycle arrest. *Cell Host Microbe* **9**:103-  
601 114.
- 602 50. **Sanders, R. L., C. L. Clark, C. S. Morello, and D. H. Spector.** 2008. Development of  
603 cell lines that provide tightly controlled temporal translation of the human  
604 cytomegalovirus IE2 proteins for complementation and functional analyses of growth-  
605 impaired and nonviable IE2 mutant viruses. *J Virol* **82**:7059-7077.

- 606 51. **Schust, J., B. Sperl, A. Hollis, T. U. Mayer, and T. Berg.** 2006. Stattic: a small-  
607 molecule inhibitor of STAT3 activation and dimerization. *Chemistry & biology* **13**:1235-  
608 1242.
- 609 52. **Sen, N., X. Che, J. Rajamani, L. Zerboni, P. Sung, J. Ptacek, and A. M. Arvin.** 2012.  
610 Signal transducer and activator of transcription 3 (STAT3) and survivin induction by  
611 varicella-zoster virus promote replication and skin pathogenesis. *Proc Natl Acad Sci U S*  
612 *A* **109**:600-605.
- 613 53. **Siddiquee, K., S. Zhang, W. C. Guida, M. A. Blaskovich, B. Greedy, H. R.**  
614 **Lawrence, M. L. Yip, R. Jove, M. M. McLaughlin, N. J. Lawrence, S. M. Sebti, and**  
615 **J. Turkson.** 2007. Selective chemical probe inhibitor of Stat3, identified through  
616 structure-based virtual screening, induces antitumor activity. *Proc Natl Acad Sci U S A*  
617 **104**:7391-7396.
- 618 54. **Sinzger, C., G. Hahn, M. Digel, R. Katona, K. L. Sampaio, M. Messerle, H. Hengel,**  
619 **U. Koszinowski, W. Brune, and B. Adler.** 2008. Cloning and sequencing of a highly  
620 productive, endotheliotropic virus strain derived from human cytomegalovirus TB40/E. *J*  
621 *Gen Virol* **89**:359-368.
- 622 55. **Slinger, E., D. Maussang, A. Schreiber, M. Siderius, A. Rahbar, A. Fraile-Ramos, S.**  
623 **A. Lira, C. Soderberg-Naucler, and M. J. Smit.** 2010. HCMV-encoded chemokine  
624 receptor US28 mediates proliferative signaling through the IL-6-STAT3 axis. *Sci Signal*  
625 **3**:ra58.
- 626 56. **Stasiak, P. C., and E. S. Mocarski.** 1992. Transactivation of the cytomegalovirus ICP36  
627 gene promoter requires the alpha gene product TRS1 in addition to IE1 and IE2. *J Virol*  
628 **66**:1050-1058.

- 629 57. **Stenberg, R. M., A. S. Depto, J. Fortney, and J. A. Nelson.** 1989. Regulated  
630 expression of early and late RNAs and proteins from the human cytomegalovirus  
631 immediate-early gene region. *J Virol* **63**:2699-2708.
- 632 58. **Tenney, D. J., and A. M. Colberg-Poley.** 1991. Human cytomegalovirus UL36-38 and  
633 US3 immediate-early genes: temporally regulated expression of nuclear, cytoplasmic,  
634 and polysome-associated transcripts during infection. *J Virol* **65**:6724-6734.
- 635 59. **Terhune, S. S., N. J. Moorman, I. M. Cristea, J. P. Savaryn, C. Cuevas-Bennett, M.**  
636 **P. Rout, B. T. Chait, and T. Shenk.** 2010. Human cytomegalovirus UL29/28 protein  
637 interacts with components of the NuRD complex which promote accumulation of  
638 immediate-early RNA. *PLoS Pathog* **6**:e1000965.
- 639 60. **Timofeeva, O. A., S. Chasovskikh, I. Lonskaya, N. I. Tarasova, L. Khavrutskii, S. G.**  
640 **Tarasov, X. Zhang, V. R. Korostyshevskiy, A. Cheema, L. Zhang, S.**  
641 **Dakshanamurthy, M. L. Brown, and A. Dritschilo.** 2012. Mechanisms of  
642 unphosphorylated STAT3 transcription factor binding to DNA. *J Biol Chem* **287**:14192-  
643 14200.
- 644 61. **Tran, K., J. P. Kamil, D. M. Coen, and D. H. Spector.** 2010. Inactivation and  
645 disassembly of the anaphase-promoting complex during human cytomegalovirus  
646 infection is associated with degradation of the APC5 and APC4 subunits and does not  
647 require UL97-mediated phosphorylation of Cdh1. *J Virol* **84**:10832-10843.
- 648 62. **Ulane, C. M., J. J. Rodriguez, J. P. Parisien, and C. M. Horvath.** 2003. STAT3  
649 ubiquitylation and degradation by mumps virus suppress cytokine and oncogene  
650 signaling. *J Virol* **77**:6385-6393.

- 651 63. **Valmas, C., M. N. Grosch, M. Schumann, J. Olejnik, O. Martinez, S. M. Best, V.**  
652 **Krahling, C. F. Basler, and E. Muhlberger.** 2010. Marburg virus evades interferon  
653 responses by a mechanism distinct from ebola virus. *PLoS Pathog* **6**:e1000721.
- 654 64. **Wang, Z., F. Luo, L. Li, L. Yang, D. Hu, X. Ma, Z. Lu, L. Sun, and Y. Cao.** 2010.  
655 STAT3 activation induced by Epstein-Barr virus latent membrane protein1 causes  
656 vascular endothelial growth factor expression and cellular invasiveness via JAK3 And  
657 ERK signaling. *Eur J Cancer* **46**:2996-3006.
- 658 65. **Weiland, K. L., N. L. Oien, F. Homa, and M. W. Wathen.** 1994. Functional analysis  
659 of human cytomegalovirus polymerase accessory protein. *Virus Res* **34**:191-206.
- 660 66. **Wen, Z., and J. E. Darnell, Jr.** 1997. Mapping of Stat3 serine phosphorylation to a  
661 single residue (727) and evidence that serine phosphorylation has no influence on DNA  
662 binding of Stat1 and Stat3. *Nucleic Acids Res* **25**:2062-2067.
- 663 67. **Wen, Z., Z. Zhong, and J. E. Darnell, Jr.** 1995. Maximal activation of transcription by  
664 Stat1 and Stat3 requires both tyrosine and serine phosphorylation. *Cell* **82**:241-250.
- 665 68. **Wilkinson, G. W., C. Kelly, J. H. Sinclair, and C. Rickards.** 1998. Disruption of  
666 PML-associated nuclear bodies mediated by the human cytomegalovirus major  
667 immediate early gene product. *J Gen Virol* **79 ( Pt 5)**:1233-1245.
- 668 69. **Yang, F., T. E. Van Meter, R. Buettner, M. Hedvat, W. Liang, C. M. Kowolik, N.**  
669 **Mepani, J. Mirosevich, S. Nam, M. Y. Chen, G. Tye, M. Kirschbaum, and R. Jove.**  
670 2008. Sorafenib inhibits signal transducer and activator of transcription 3 signaling  
671 associated with growth arrest and apoptosis of medulloblastomas. *Mol Cancer Ther*  
672 **7**:3519-3526.

- 673 70. **Yang, J., M. Chatterjee-Kishore, S. M. Staugaitis, H. Nguyen, K. Schlessinger, D. E.**  
674 **Levy, and G. R. Stark.** 2005. Novel roles of unphosphorylated STAT3 in oncogenesis  
675 and transcriptional regulation. *Cancer Res* **65**:939-947.
- 676 71. **Yang, J., X. Liao, M. K. Agarwal, L. Barnes, P. E. Auron, and G. R. Stark.** 2007.  
677 Unphosphorylated STAT3 accumulates in response to IL-6 and activates transcription by  
678 binding to NFkappaB. *Genes Dev* **21**:1396-1408.
- 679 72. **Yoo, J. Y., D. L. Huso, D. Nathans, and S. Desiderio.** 2002. Specific ablation of  
680 Stat3beta distorts the pattern of Stat3-responsive gene expression and impairs recovery  
681 from endotoxic shock. *Cell* **108**:331-344.
- 682 73. **Yu, D., G. A. Smith, L. W. Enquist, and T. Shenk.** 2002. Construction of a self-  
683 excisable bacterial artificial chromosome containing the human cytomegalovirus genome  
684 and mutagenesis of the diploid TRL/IRL13 gene. *J Virol* **76**:2316-2328.
- 685 74. **Yu, H., M. Kortylewski, and D. Pardoll.** 2007. Crosstalk between cancer and immune  
686 cells: role of STAT3 in the tumour microenvironment. *Nat Rev Immunol* **7**:41-51.
- 687 75. **Yu, H., D. Pardoll, and R. Jove.** 2009. STATs in cancer inflammation and immunity: a  
688 leading role for STAT3. *Nat Rev Cancer* **9**:798-809.
- 689 76. **Zammarchi, F., E. de Stanchina, E. Bournazou, T. Supakorndej, K. Martires, E.**  
690 **Riedel, A. D. Corben, J. F. Bromberg, and L. Cartegni.** 2011. Antitumorigenic  
691 potential of STAT3 alternative splicing modulation. *Proc Natl Acad Sci U S A*  
692 **108**:17779-17784.

693

694 **FIGURE LEGENDS**

695 **Figure 1. Infection increases the levels of unphosphorylated STAT3 in the nucleus and**  
696 **inhibits IL6-stimulated gene expression.**

697 (A) Serum-starved U373 cells were mock-infected or infected with AD<sub>wt</sub> at 5 IU/cell in 0.5%  
698 serum. Samples were fixed at the indicated times, incubated with antibodies against STAT3  
699 (green) and pSTAT3 at Y705 (red), and counterstained for DNA with DAPI (blue). Where  
700 indicated, mock samples were treated with IL6 at 183 ng/ml. The mean fluorescent intensity of  
701 STAT3 within the nucleus and cytoplasm was obtained from an average of 20-30 cells and from  
702 at least two replicate experiments. The data is presented as nuclear to cytoplasmic ratio  $\pm$  SEM.  
703 (B) Cells were infected as above and treated with IL6 or DMSO for 15 min prior to Western blot  
704 analysis using the indicated antibodies. The  $\alpha$ - and  $\beta$ -STAT3 isoforms are evident upon  
705 sufficient electrophoretic separation.  
706 (C) The above experiment was repeated using the clinical isolate TB40/E.  
707 (D) Cells were infected at 1 IU/cell and treated with IL6 or DMSO for 45 min just prior to  
708 harvest at 24 and 48 hpi. Levels of the indicated mRNAs were quantified by qRT-PCR and  
709 presented relative to GAPDH. Data represent two biological replicate experiments and are  
710 presented as the mean  $\pm$  SEM (\*p < 0.05).

711 (E) Serum-starved U373 cells were infected as described in (A). Cells were fixed, stained with  
712 anti-IL6R $\alpha$  antibody conjugate to Alexa-Fluor 647 and analyzed using flow cytometry. As a  
713 control, cells were treated with trypsin solution for 15 min prior to antibody staining (grey) and  
714 the values represent the mean fluorescence intensity from two biological experiments.

715

716 **Figure 2. Nuclear accumulation of STAT3 reduces IL6-induced phosphorylation and is**  
717 **dependent on viral gene expression.**



718 (A) Serum-starved U373 cells were transfected with control siRNAs or an siRNA targeting  
719 importin- $\beta$ 1 24 h prior to infection. Cells were mock-infected or infected with AD $_{wt}$  virus at 5  
720 IU/cell and treated with IL6 for 15 min prior to harvest at 24 hpi. Western blot analysis was  
721 completed using the indicated antibodies.

722 (B) Cells were transfected, infected, and treated with IL6 as described above. At 24 hpi, cells  
723 were processed for immunofluorescence analysis using anti-STAT3 (green) and DAPI (blue).  
724 The mean fluorescent intensity of STAT3 within the nucleus and cytoplasm was obtained from  
725 an average of 20-30 cells and from at least two replicate experiments. The data is presented as  
726 nuclear to cytoplasmic ratio  $\pm$  SEM.

727 (C) U373 cells were mock-infected or infected at 5 IU/cell with either untreated or UV-irradiated  
728 AD $_{wt}$  virus. At 5 hpi, cells were processed for immunofluorescence analysis using anti-STAT3  
729 (green) and DAPI (blue). The mean fluorescent intensity of STAT3 within the nucleus and  
730 cytoplasm was determined as described above.

731 (D) U373 cells were mock-infected or infected at 5 IU/cell with either untreated or UV-irradiated  
732 AD $_{wt}$  virus. At 5 hpi, cells were harvested and levels of IE1 mRNA was quantified by qRT-PCR  
733 and presented relative to GAPDH. Data represent two biological replicate experiments and are  
734 presented as the mean  $\pm$  SEM.

735

736 **Figure 3. HCMV IE1 interacts with STAT3 and promotes STAT3 nuclear accumulation.**

737 (A) Growth-arrested MRC-5 cells were mock-infected or infected with *wt* or *dIE1* at 3 PFU/cell  
738 in 10% serum. Samples were fixed at the indicated times, incubated with antibodies against  
739 STAT3 (green) and HCMV IE2 (red), and counterstained for DNA using DAPI (blue). Scale bar,  
740 10  $\mu$ m. The mean fluorescent intensity of STAT3 within the nucleus and cytoplasm was obtained

741 from an average of 100 cells. The data is presented as mean nuclear to cytoplasmic ratio  $\pm$   
742 standard deviation.

743 (B) Cells were infected with *wt* or *dIE1* at 3 PFU/cell. Samples were fixed at 48 hpi and stained  
744 as described in (A). STAT3 staining of IE2-positive mitotic cells (left set of panels) or STAT3  
745 colocalization with IE1 at mitotic chromatin (right set of panels) is shown. Scale bars, 10  $\mu$ m.

746 (C) Cells were infected as described in (B) and extracts isolated at 24 hpi. Samples were  
747 subjected to immunoprecipitation using antibodies to IE1 or IE2 and Western blot analysis was  
748 completed on lysate and IP samples using the indicated antibodies.

749 (D) Cells were infected as described in (B) and extracts isolated at 6 to 72 hpi. Samples were  
750 subjected to immunoprecipitation using an antibody to STAT3 or normal rabbit IgG and Western  
751 blot analysis was completed on lysates and IP samples using the indicated antibodies.

752

753 **Figure 4. HCMV IE1 inhibits STAT3 phosphorylation, DNA binding and target gene**  
754 **expression.**

755 (A) Serum-starved MRC-5 cells were infected with *wt* or *dIE1* at 3 PFU/cell and treated with  
756 IL6 and IL6R $\alpha$  or solvent. Samples from 16 hpi were subjected to Western blot analysis using  
757 the indicated antibodies.

758 (B) Serum-starved cells were infected as described in (A) and treated with IL6 and IL6R $\alpha$  or  
759 solvent for 30 min. Samples from 16 hpi were subjected to ChIP using an antibody to STAT3 or  
760 normal rabbit IgG and primers specific for sequences in the SOCS3 promoter or transcribed  
761 region. The percentage of output to input DNA was calculated and is presented as the difference  
762 between STAT3 and normal IgG ChIPs. Data represent two biological and two technical  
763 replicates, and values are given as the mean  $\pm$  standard deviation.

764 (C) Serum-starved cells were infected and treated as described in (A). Relative SOCS3 and IE2  
765 mRNA levels at 16 hpi were determined by qRT-PCR and presented relative to TUBB  
766 expression. Data represent three biological and two technical replicates, and values are given as  
767 the mean  $\pm$  standard deviation.

768

769 **Figure 5. IE1 is sufficient to alter STAT3 localization and to inhibit STAT3**  
770 **phosphorylation, DNA binding and target gene expression.**

771 (A) TetR-IE1 and TetR cells were treated with doxycycline (Dox) for 0 to 72 h and 72 h,  
772 respectively. Samples were fixed, incubated with antibodies against IE1 (green) and STAT3  
773 (red), and counterstained for DNA using DAPI (blue). Scale bar, 10  $\mu$ m.

774 (B) The percentage of positive cell nuclei was determined from 100 randomly selected cells per  
775 sample (IE1 -, no IE1 staining above background; IE1 +, weak, mostly punctate IE1 staining;  
776 IE1 ++, strong, diffuse IE1 staining; STAT3 -, STAT3 staining mostly cytoplasmic; STAT3 +,  
777 STAT3 staining cytoplasmic and nuclear; STAT3 ++, STAT3 staining mostly nuclear).

778 (C) TetR-IE1 and TetR cells were treated with Dox. Samples were fixed at 48 hpi and stained as  
779 described in (A). Representative mitotic cells are shown. Scale bar, 10  $\mu$ m.

780 (D) TetR-IE1 cells were treated with Dox for 0 to 72 h and Western blot analysis was completed  
781 using the indicated antibodies.

782 (E) TetR-IE1 and TetR cells were treated with Dox for 0 to 72 h. Relative SOCS3 mRNA levels  
783 were determined by qRT-PCR and presented relative to TUBB expression and TetR at time 0 h.  
784 Data represent two biological and two technical replicates, and values are given as the mean  $\pm$   
785 standard deviation.

786 (F) TetR-IE1 and TetR cells were treated with Dox for 72 h and with IL6 and IL6R $\alpha$  or solvent.  
787 Western blot analysis was completed using the indicated antibodies.

788 (G) TetR-IE1 and TetR cells were treated with Dox for 72 h and with IL6 and IL6R $\alpha$  or solvent  
789 for 30 min. Samples were subjected to ChIP using an antibody to STAT3 or normal rabbit IgG  
790 and primers specific for sequences in the SOCS3 promoter or transcribed region. The percentage  
791 of output to input DNA was calculated and is presented as the difference between STAT3 and  
792 normal IgG ChIPs. Data represent two biological and two technical replicates, and values are  
793 given as the mean  $\pm$  standard deviation. \*, below detection limit.

794 (H) TetR and TetR-IE1 cells were treated with Dox for 72 h and with IL6 and IL6R $\alpha$  or solvent.  
795 Relative SOCS3 mRNA levels were determined by qRT-PCR and presented relative to TUBB  
796 expression and TetR. Data represent three biological and two technical replicates, and values are  
797 given as the mean  $\pm$  standard deviation.

798

799 **Figure 6. Chemical disruption of STAT3 inhibits HCMV replication.**

800 (A) U373 cells were treated with increasing concentrations of S3i-201, curcumin, STATTIC, or  
801 WP1066. At 72 h, cell viability was quantified. The data represent two biological replicate  
802 experiments and are presented as the mean  $\pm$  SEM.

803 (B) Cells were pretreated with DMSO, S3i-201, curcumin, STATTIC, or WP1066. After 24 h,  
804 cells were infected at 5 IU/cell using AD $_{wt}$  and processed for immunofluorescence analysis  
805 using an antibody to STAT3 (green) and the DNA stain DAPI (blue). The mean fluorescent  
806 intensity of STAT3 within the nucleus and cytoplasm was obtained from an average of 20-30  
807 cells and from at least two biological replicate experiments. The data is presented as nuclear to  
808 cytoplasmic ratio  $\pm$  SEM.

809 (C) Cells were pretreated with drug as described above. After 24 h, cells were infected at 0.25  
810 IU/cell using AD $wt$ . Viral genomes were quantified at 72 hpi by qPCR and normalized to  
811 cellular DNA. Data represent two biological replicates and values are given as the mean  $\pm$  SEM  
812 (\* $p < 0.05$ ).

813

814 **Figure 7. S3i-201 inhibits HCMV replication in multiple different cell types.**

815 (A) Cells were pretreated with increasing concentrations of S3i-201. After 24 h, cells were  
816 infected at 0.25 IU/cell using AD $wt$ . Viral genomes were quantified at 72 hpi by qPCR and  
817 normalized to cellular DNA. Data represent two biological replicates and values are given as the  
818 mean  $\pm$  SEM (\* $p < 0.05$ ).

819 (B) U373 cells were pretreated with 125  $\mu$ M of S3i-201. After 24 h, cells were infected at 3  
820 IU/cell using AD $wt$ . Viral genomes were quantified as described above. Data represent two  
821 biological replicates, and values are given as the mean  $\pm$  SEM (\* $p < 0.05$ ).

822 (C) Different cell types were pretreated with 125  $\mu$ M of S3i-201. U373 and HFF cells were  
823 infected at 0.25 IU/cell using AD $wt$  while ARPE19 cells were infected at 0.25 IU/cell using  
824 TB40/E. Viral genomes were quantified as above. Data represent two biological replicates, and  
825 values are given as the mean  $\pm$  SEM (\* $p < 0.05$ ).

826 (D) U373 cells were pretreated with drug as described above. At 24 h, cells were infected at 0.25  
827 IU/cell using AD $wt$ . Viral titers were determined from culture supernatants obtained at 96 hpi.  
828 Data represent two biological replicates, and values are given as the mean  $\pm$  SEM (\* $p < 0.05$ ).

829

830 **Figure 8. siRNA targeting STAT3 attenuates viral DNA replication.**

831 (A) Serum-starved U373 cells were transfected with control siRNA or siRNA targeting STAT3.  
832 After 24 h, Western blot analysis was completed using the indicated antibodies.

833 (B) Cells were transfected as described above. After 24 h, cells were processed for  
834 immunofluorescence analysis using anti-STAT3 (green) and DAPI (blue). The mean fluorescent  
835 intensity of STAT3 within the nucleus and cytoplasm was obtained from an average of 20-30  
836 cells and from at least two replicate experiments. The data is presented as nuclear to cytoplasmic  
837 ratio  $\pm$  SEM.

838 (C) Cells were transfected as described above. After 24 hr, cells were infected with AD<sub>wt</sub> virus  
839 at 0.25 IU/cell. Viral genomes were quantified at 72 hpi by qPCR and normalized to cellular  
840 DNA. Data represent two biological replicates and values are given as the mean  $\pm$  SEM (\*p <  
841 0.05).

842

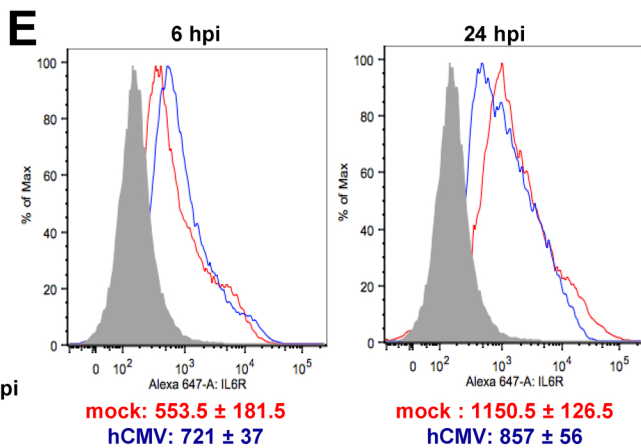
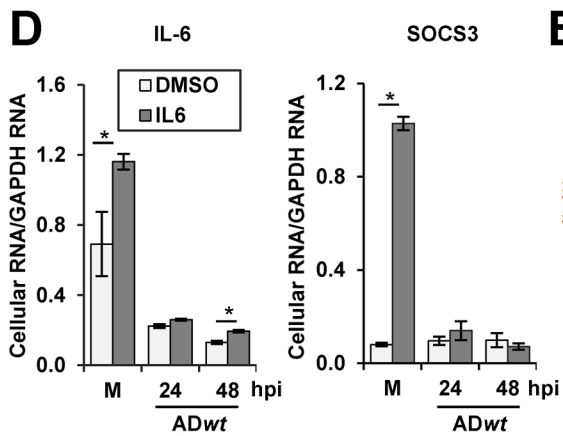
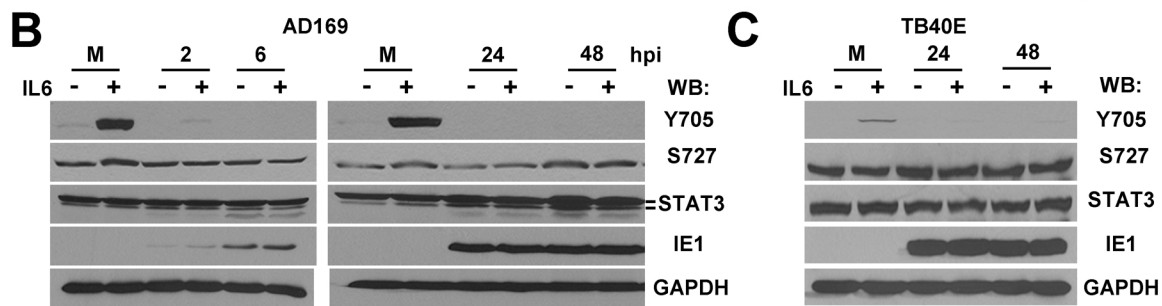
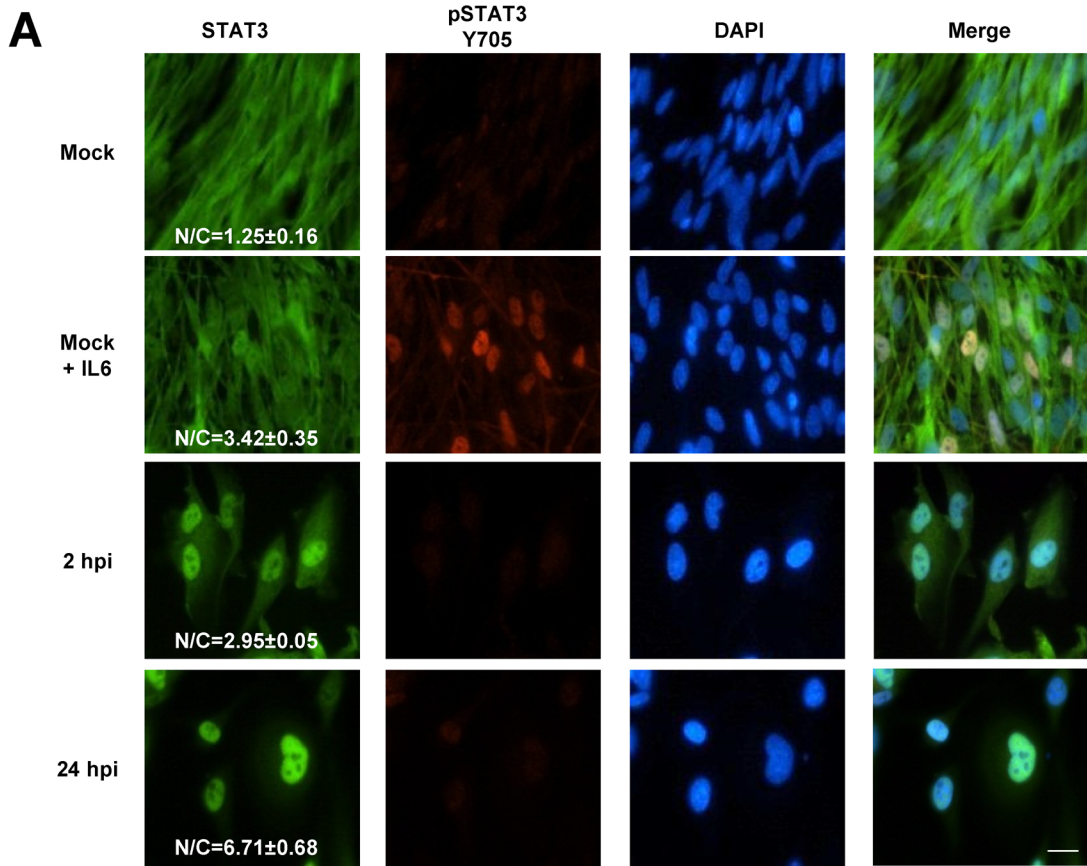
843 **Figure 9 STAT3 is necessary for efficient HCMV gene expression and genome replication.**

844 (A) U373 cells were pretreated with DMSO or 125  $\mu$ M of S3i-201. After 24 h, cells were  
845 infected at 0.25 IU/cell using AD<sub>wt</sub>. Levels of the indicated RNAs were quantified by qRT-PCR  
846 and presented relative to GAPDH. Data represent two biological replicate experiments, and  
847 values are given as the mean  $\pm$  SEM (\*p < 0.05).

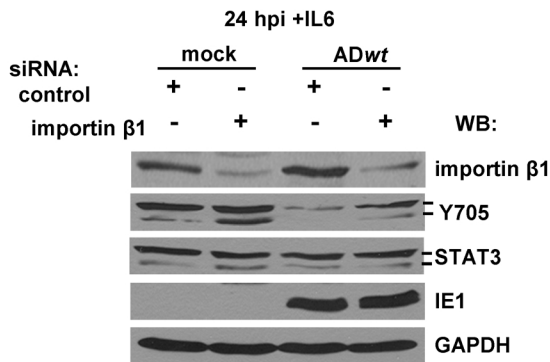
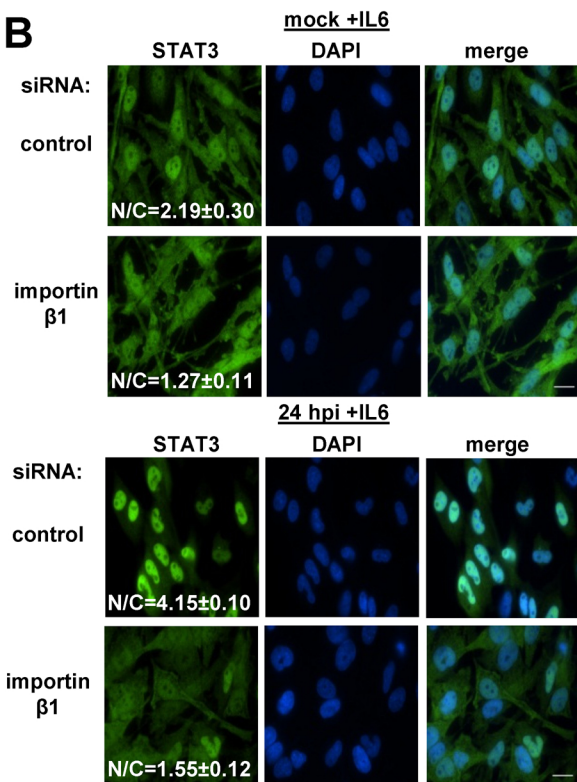
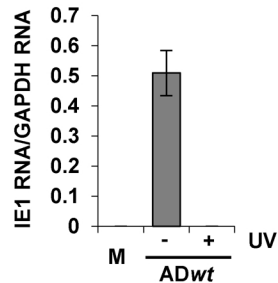
848 (B) U373 cells were pretreated with drug as described above, and after 24 h cells were infected  
849 for 2 to 72 h with AD<sub>wt</sub> at 0.25 IU/cell. Western blot analysis was completed using the indicated  
850 antibodies.

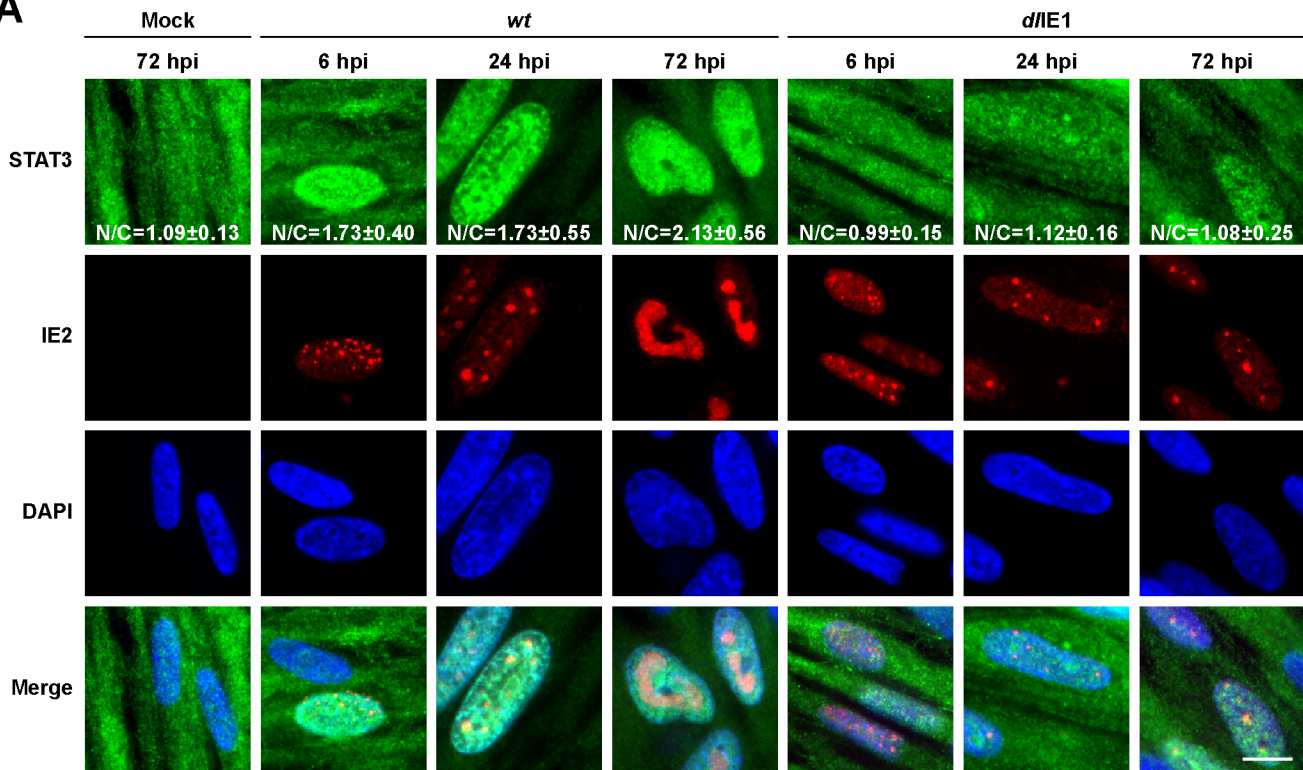
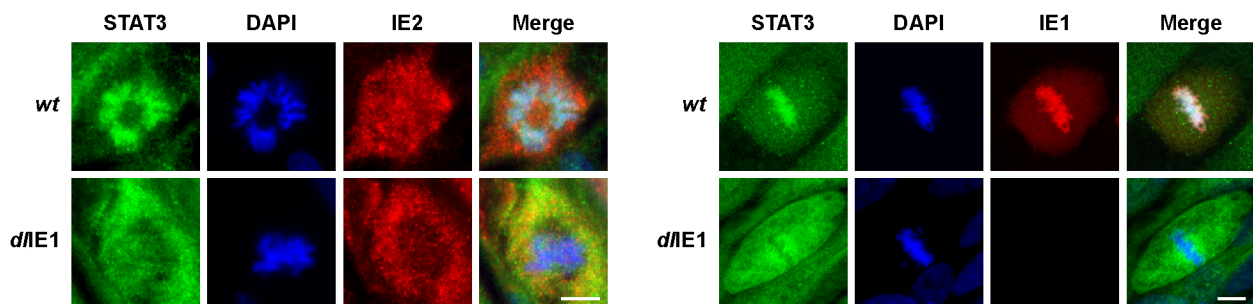
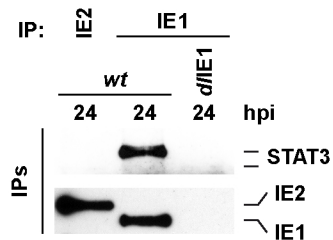
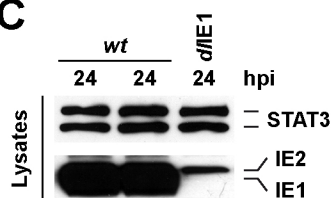
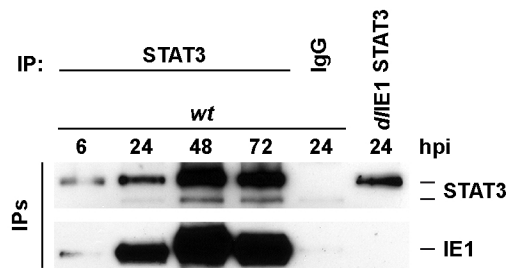
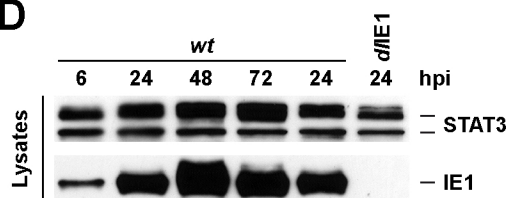
851 (C) U373 cells were infected at 0.25 IU/cell using AD<sub>wt</sub>. Cells were then treated for 24 h with  
852 125  $\mu$ M of S3I-201 at either 2 hpi or 48 hpi. After 72 hpi, viral genomes were quantified by

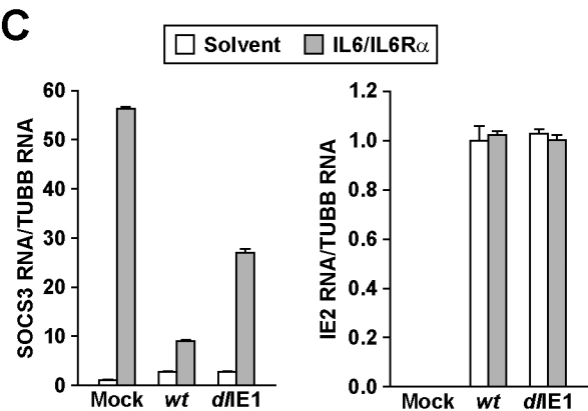
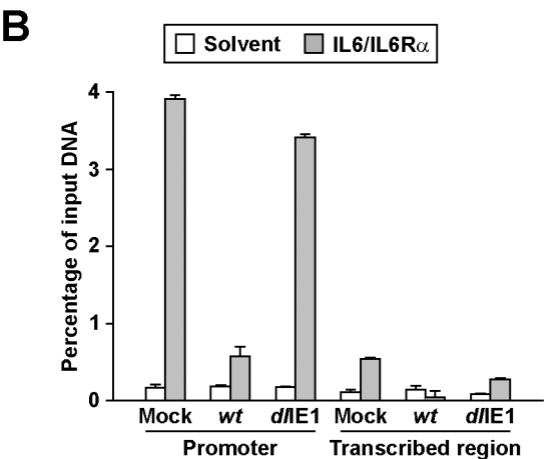
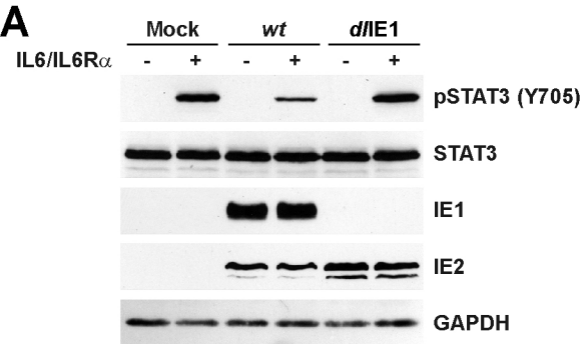
853 qPCR and normalized to cellular DNA. Data represent two biological replicates, and values are  
854 given as the mean  $\pm$  SEM (\*p < 0.05).

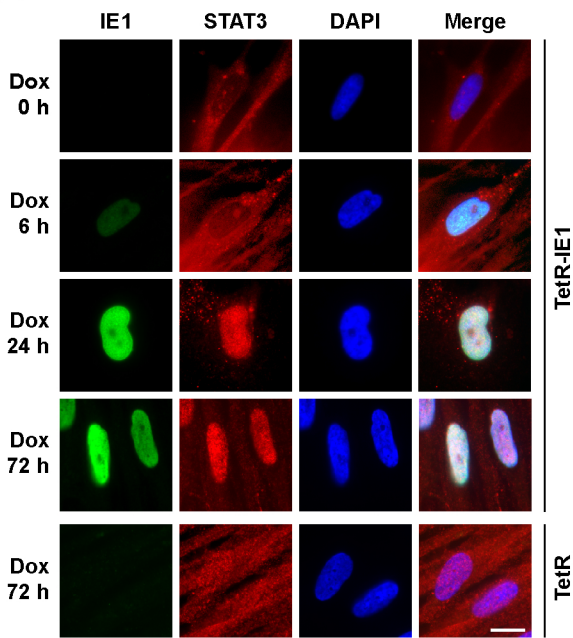
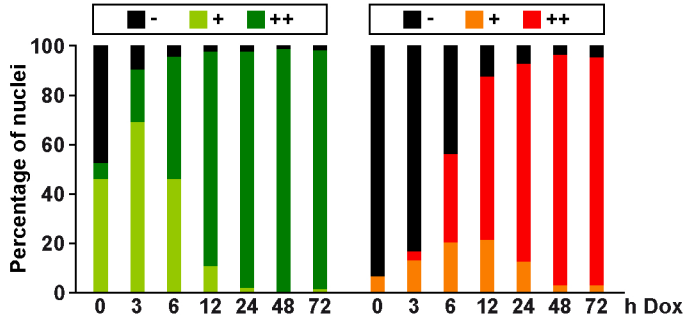
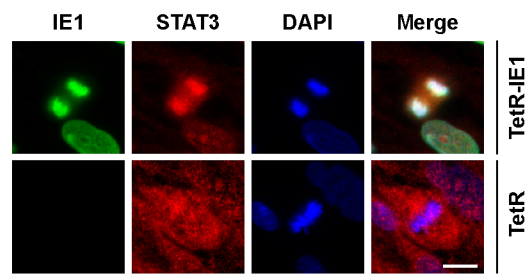
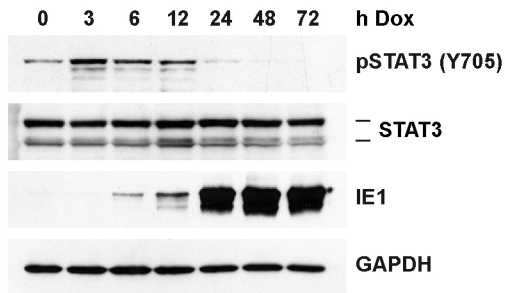
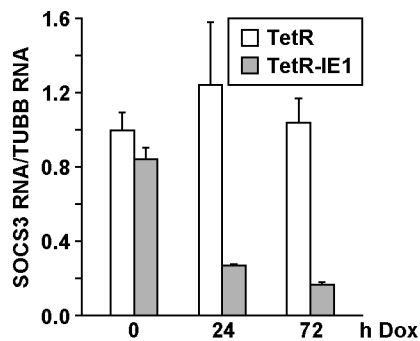
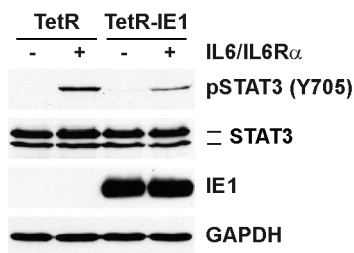
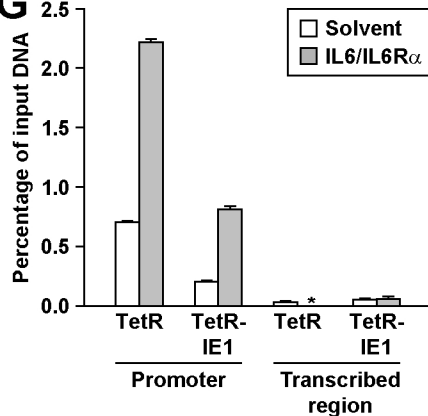
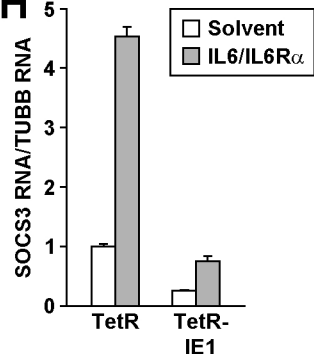


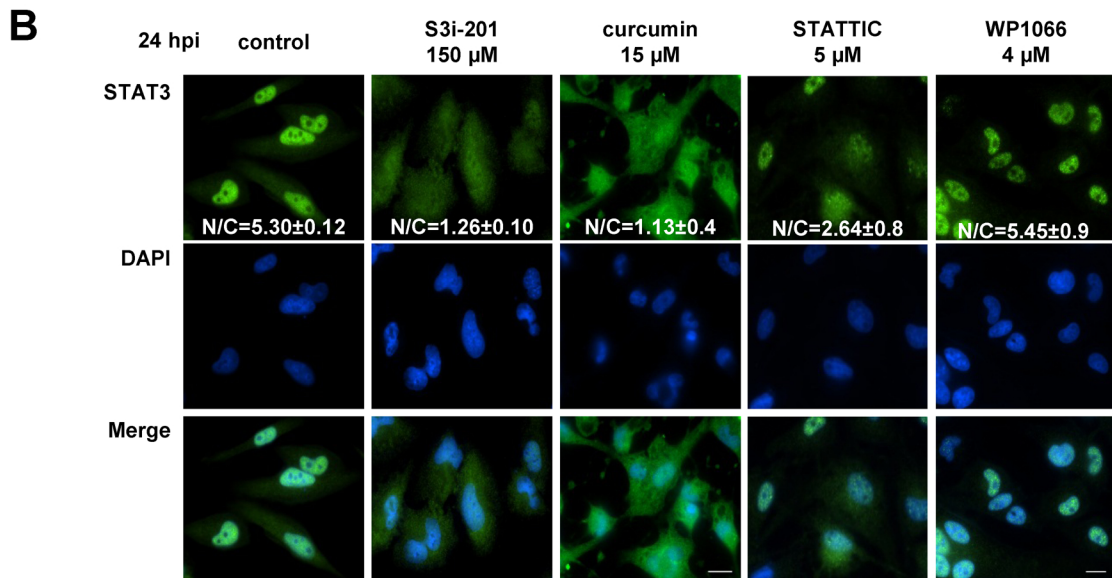
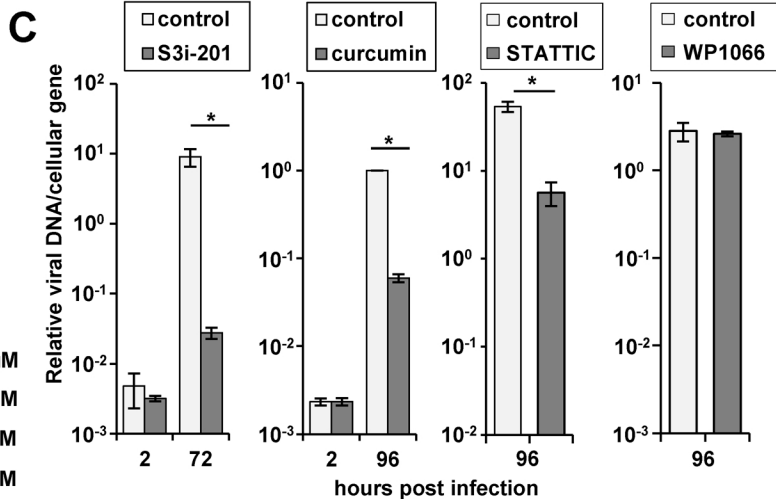
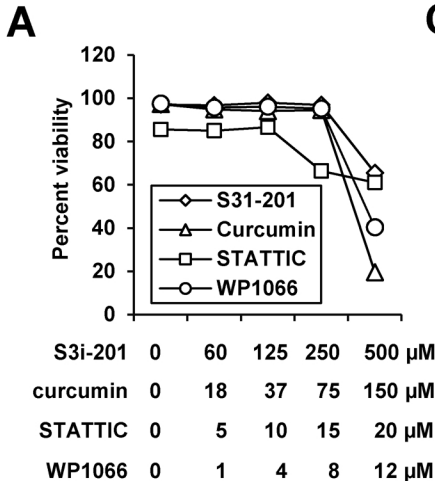


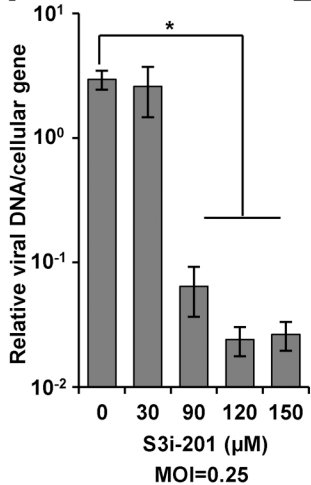
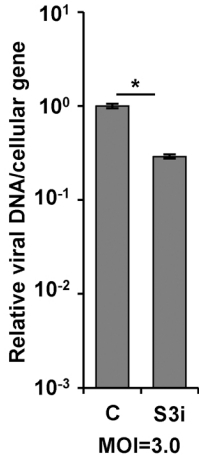
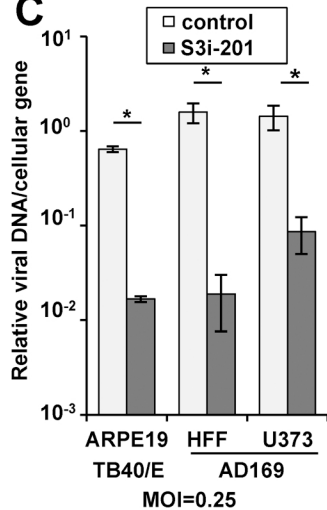
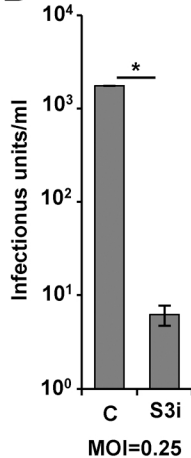
**A****B****D**

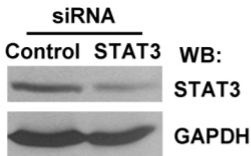
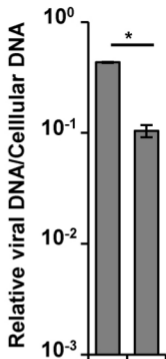
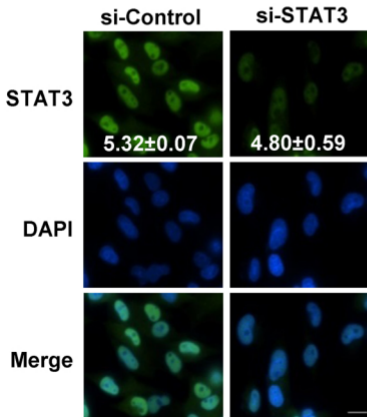
**A****B****C****D**



**A****B****C****D****E****F****G****H**



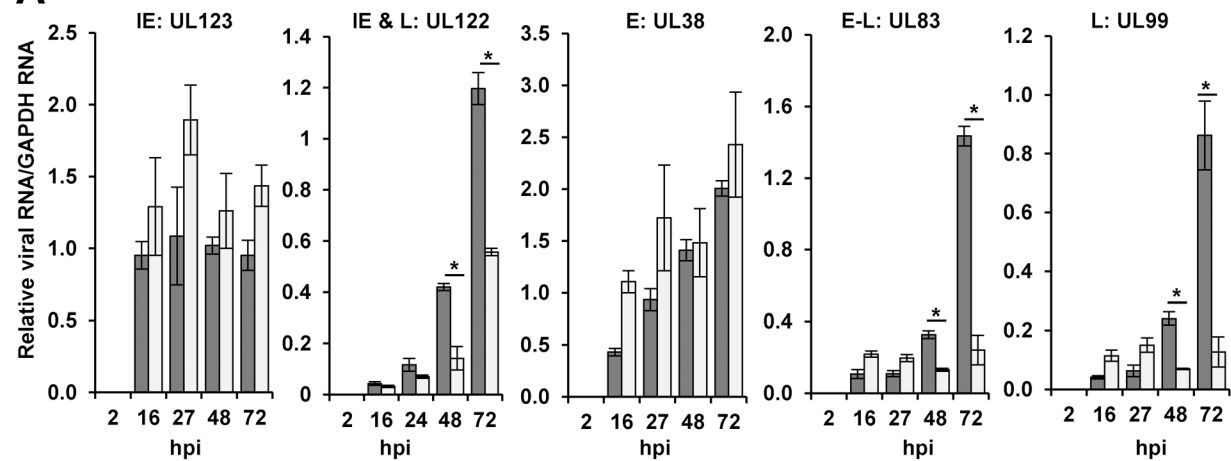
**A****B****C****D**

**A****C****B**

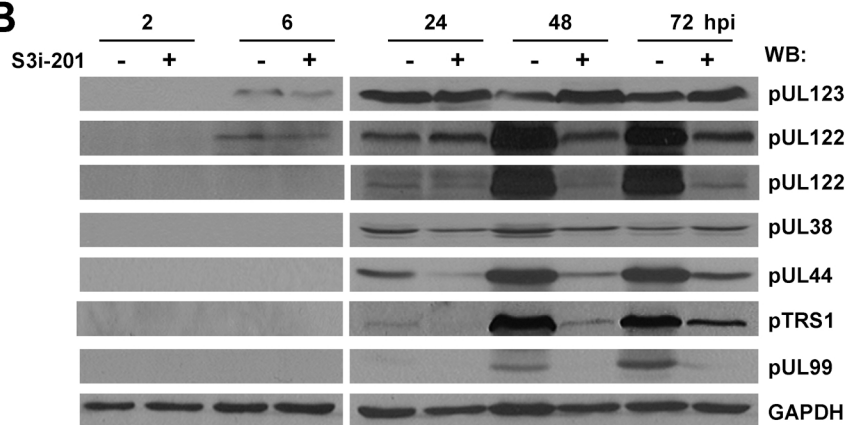
si-Control	+	-
si-STAT3	-	+

■ ADwt    □ ADwt +S3i-201

**A**



**B**



**C**

